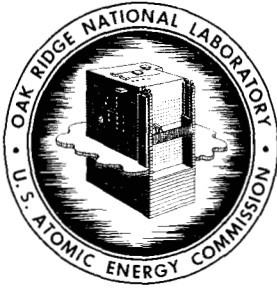


ORNL
MASTER COPY



OAK RIDGE NATIONAL LABORATORY

operated by

UNION CARBIDE CORPORATION
NUCLEAR DIVISION



for the

U.S. ATOMIC ENERGY COMMISSION

ORNL - TM - 3014

AUG 18 1970

DATE ISSUED: _____

67

PHASE REPORT NO. 115-1

on

STRESS INDICES FOR SMALL BRANCH
CONNECTIONS WITH EXTERNAL LOADINGS

E. C. Rodabaugh

Battelle Memorial Institute

NOTICE This document contains information of a preliminary nature and was prepared primarily for internal use at the Oak Ridge National Laboratory. It is subject to revision or correction and therefore does not represent a final report.

LEGAL NOTICE

This report was prepared as an account of Government sponsored work. Neither the United States, nor the Commission, nor any person acting on behalf of the Commission:

- A. Makes any warranty or representation, expressed or implied, with respect to the accuracy, completeness, or usefulness of the information contained in this report, or that the use of any information, apparatus, method, or process disclosed in this report may not infringe privately owned rights; or
- B. Assumes any liabilities with respect to the use of, or for damages resulting from the use of any information, apparatus, method, or process disclosed in this report.

As used in the above, "person acting on behalf of the Commission" includes any employee or contractor of the Commission, or employee of such contractor, to the extent that such employee or contractor of the Commission, or employee of such contractor prepares, disseminates, or provides access to, any information pursuant to his employment or contract with the Commission, or his employment with such contractor.

ORNL-TM-3014

Contract No. W-7405-eng-26

Reactor Division

PHASE REPORT NO. 115-1

on

STRESS INDICES FOR SMALL BRANCH
CONNECTIONS WITH EXTERNAL LOADINGS

E. C. Rodabaugh

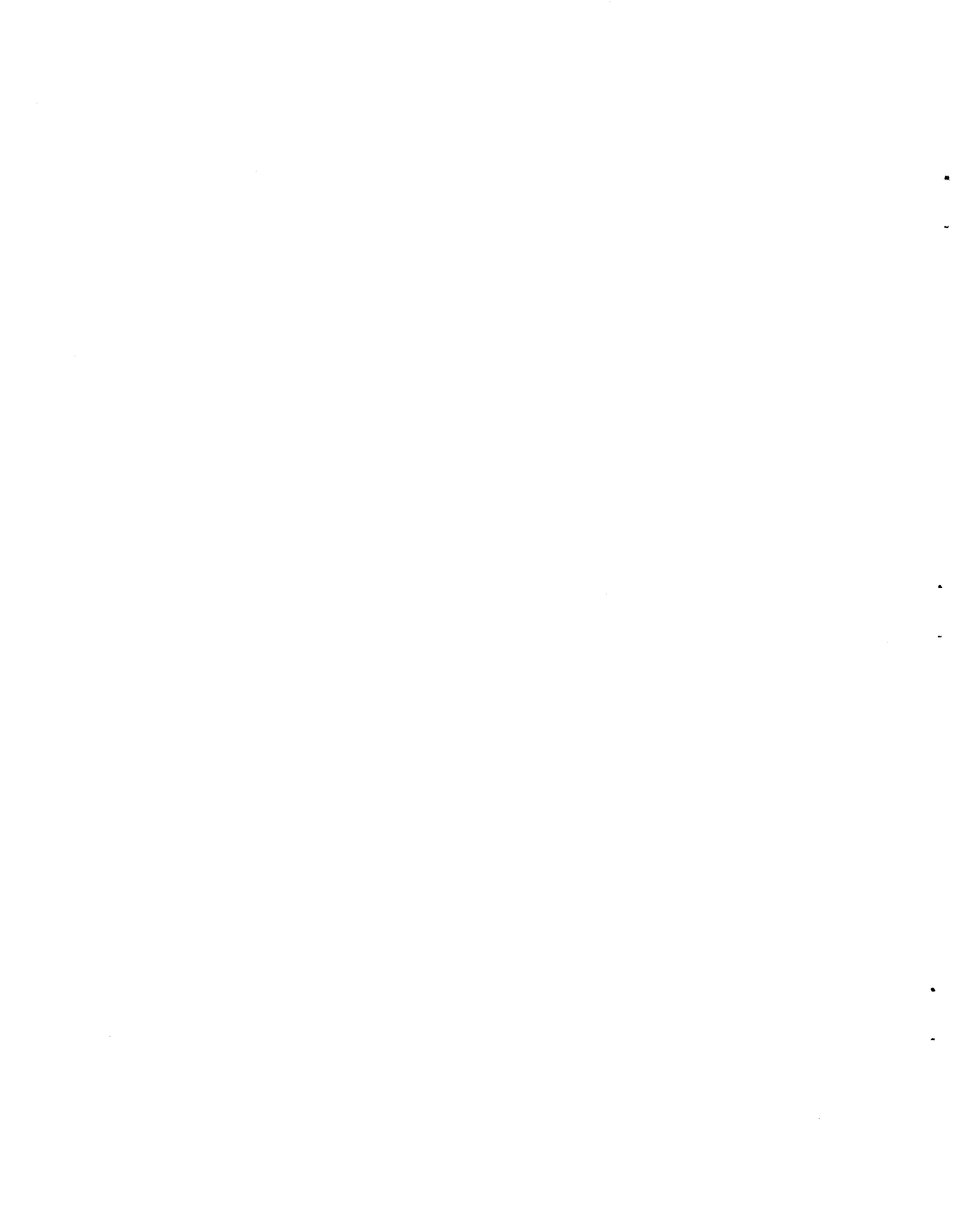
Battelle Memorial Institute

AUGUST 1970

Subcontract No. 2913

for

OAK RIDGE NATIONAL LABORATORY
Oak Ridge, Tennessee
operated by
UNION CARBIDE CORPORATION
for the
U.S. ATOMIC ENERGY COMMISSION



FOREWORD

The work reported here was done at Battelle Memorial Institute under subcontract to the Oak Ridge National Laboratory (ORNL) which is operated by Union Carbide Corporation for the U.S. Atomic Energy Commission. This effort is part of the "Design Criteria for Piping, Pumps, and Valves Program" (ORNL Piping Program) under the direction of W. L. Greenstreet, Head, Applied Mechanics Section, and S. E. Moore, Program Coordinator. The ORNL Piping Program is the AEC supported portion of an AEC-Industry cooperative effort for the development of design criteria for piping components, pumps, and valves to be used in nuclear power plant piping systems. The AEC-Industry cooperative effort is coordinated by the Pressure Vessel Research Committee (PVRC) of the Welding Research Council. J. L. Mershon is the USAEC cognizant engineer.

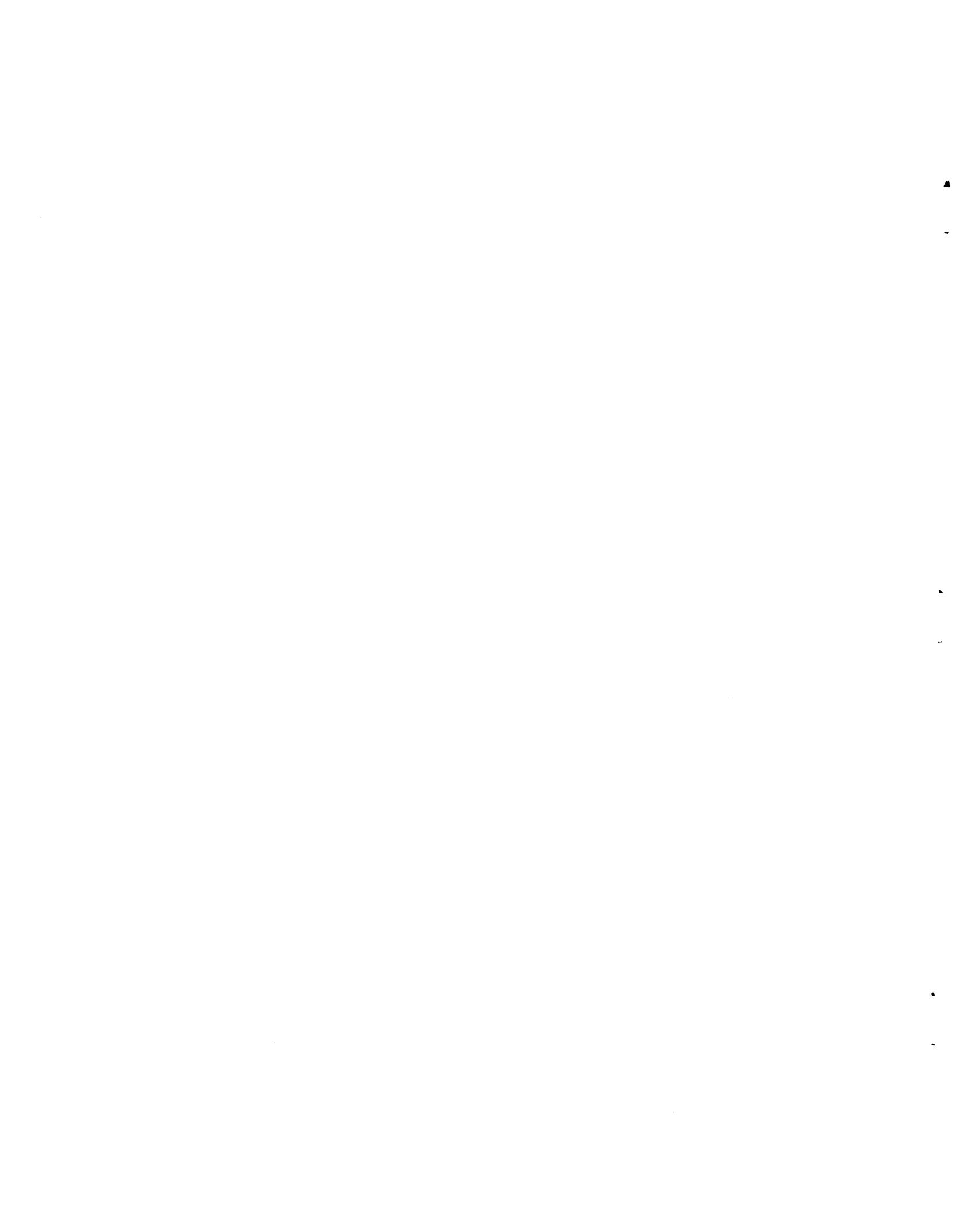


TABLE OF CONTENTS

	<u>Page</u>
NOMENCLATURE	vi
ABSTRACT	1
INTRODUCTION	2
LOADINGS AND STRESS INDICES	4
TEST DATA	14
PROPOSED INDICES FOR B31.7	28
Moment Loading Thru Branch	28
Moment Loading Thru Run	35
Resultant Moment	40
B ₂ -indices	41
Summary and Example	43
STRESSES BY B31.1.0 POWER PIPING CODE	48
FORCE LOADINGS	51
RECOMMENDED CHANGES IN B31.7	56
REFERENCES	61

NOMENCLATURE

d = branch pipe diameter

D = run pipe diameter

t = run pipe wall thickness

(Other dimensional symbols are defined in Figure 1)

θ, ρ = coordinates of point on branch connections; See Figure 3.

M_{ij} ; where $i = x, y, z, j = 1, 2, 3$
Set of nine orthogonal moments given by a piping system flexibility analysis; See Figure 2.

F_{ij} ; as above, except forces

M_{ij} ; where $i = x, y, z, j = r, b$
Set of six independent orthogonal moments used in the test arrangement shown in Figure 3.

L = axial force applied to branch pipe

Z = section modulus of pipe

A = cross sectional metal area of pipe

Z_b = section modulus of branch pipe

Z_r = section modulus of run pipe

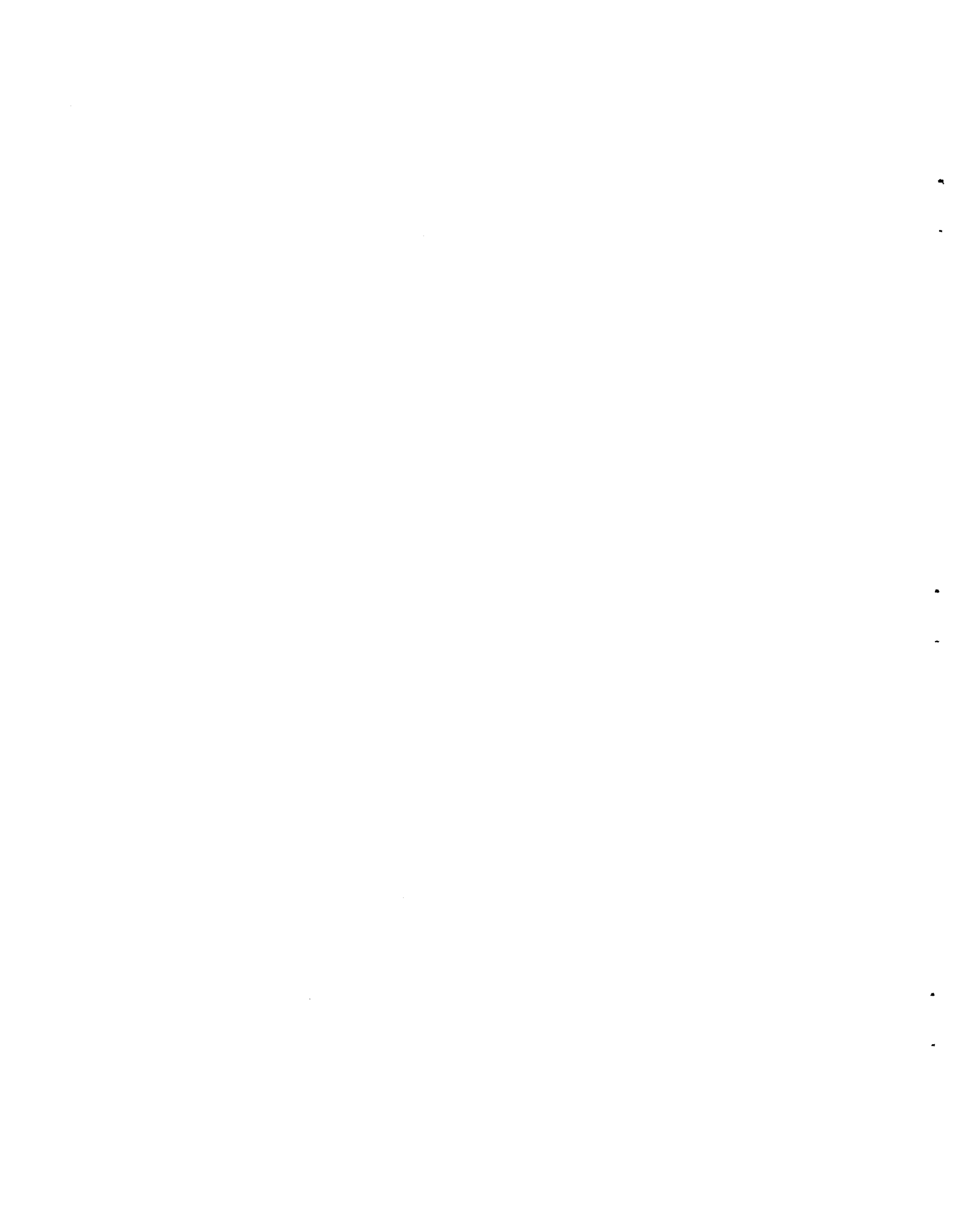
C, i = (with various subscripts) are stress indices

S = a nominal stress

σ = a specific principal stress in a branch connection

$\bar{\sigma}$ = a specific stress intensity in a branch connection

Additional symbols are defined in the text as they occur.



STRESS INDICES FOR SMALL BRANCH
CONNECTIONS WITH EXTERNAL LOADINGS

E. C. Rodabaugh

ABSTRACT

Stress indices and simplified design formulas are developed for use in the stress analysis of small branch connections in Class I piping systems as required by the ANSI Standard, Code for Pressure Piping, Nuclear Power Piping ANSI B31.7. Equations are given for reducing the set of nine moments which act on a branch connection, and whose numerical values are obtained from a piping flexibility analysis to two resultant moments. Stress indices to be used with these resultant moments are empirically developed from existing test data; and design rules are proposed for inclusion in ANSI B31.7. The effects of direct shear force loadings on branch connections are also discussed.

Keywords: stress indices, small branch connections, piping tees, stress analysis, nuclear piping, piping code, ANSI B31.7.

INTRODUCTION

The Nuclear Power Piping Code, USAS B31.7⁽¹⁾, provides stress indices for two* broad types of branch connections:

- 1) Branch connections per Subpar. 1-704.3.
- 2) Butt-welding tees per USAS B16.9 or MSS SP-48.

This Phase Report is concerned only with the first type of branch connections. It should be remarked that the first type of branch connections are assigned stress indices in Table D201 of B31.7 only for $d/D \leq 0.5$, where d = branch diameter, D = run diameter. In contrast, butt welding tees are normally available only for $d/D > \sim 0.5$. In the following, we will use the term "branch connections" as referring specifically to branch connections per Subpar. 1-704.3.

Two additional limitations are placed on the applicability of stress indices to branch connections:

- 1) D/t not over 100; t = wall thickness of run pipe.
- 2) Branch pipe axis normal to the surface of the run pipe
(For example, laterals are excluded.)

Subparagraph 1-704.3 of B31.7 is entitled "Intersections"; it requires 100% cut-out area replacement unless $d \leq 0.1414 \sqrt{Dt}$ and further provides reinforcing zone bounds within which reinforcing is considered as effective in replacing the cut-out area. The reinforcing is based on internal pressure loading only and is not related to the magnitude of the external loadings. Because essentially any branch

* A third class of branch connections consists of socket-welding fittings such as those purchased to USAS B16.11. These apparently present a design problem only at the socket weld.

connection will meet the reinforcing rules for some pressure, the present B31.7 formulation for C_2 for branch connections is subject to misapplication. The present formulation for $C_2 = 1.8 (R_m/3 T_r)^{2/3}$ is based on the assumption that T_r is the thickness of the run pipe required for internal pressure and that additional reinforcing is required to meet the B31.7 reinforcing rules. Because either part or all of the reinforcing can be supplied by the run pipe, the present formulation for C_2 may not be conservative for some configurations*.

USAS B31.1.0-1967, Power Piping, gives some equations for calculating stresses in branch connections; but is limited to (1) B16.9 tees, (2) pad or saddle reinforced tees, or (3) uniform wall (fabricated, unreinforced) tees. The first of these is not included in this report; the second is not permissible under B31.7, hence only the third type might offer some guidance. These code rules are discussed later herein.

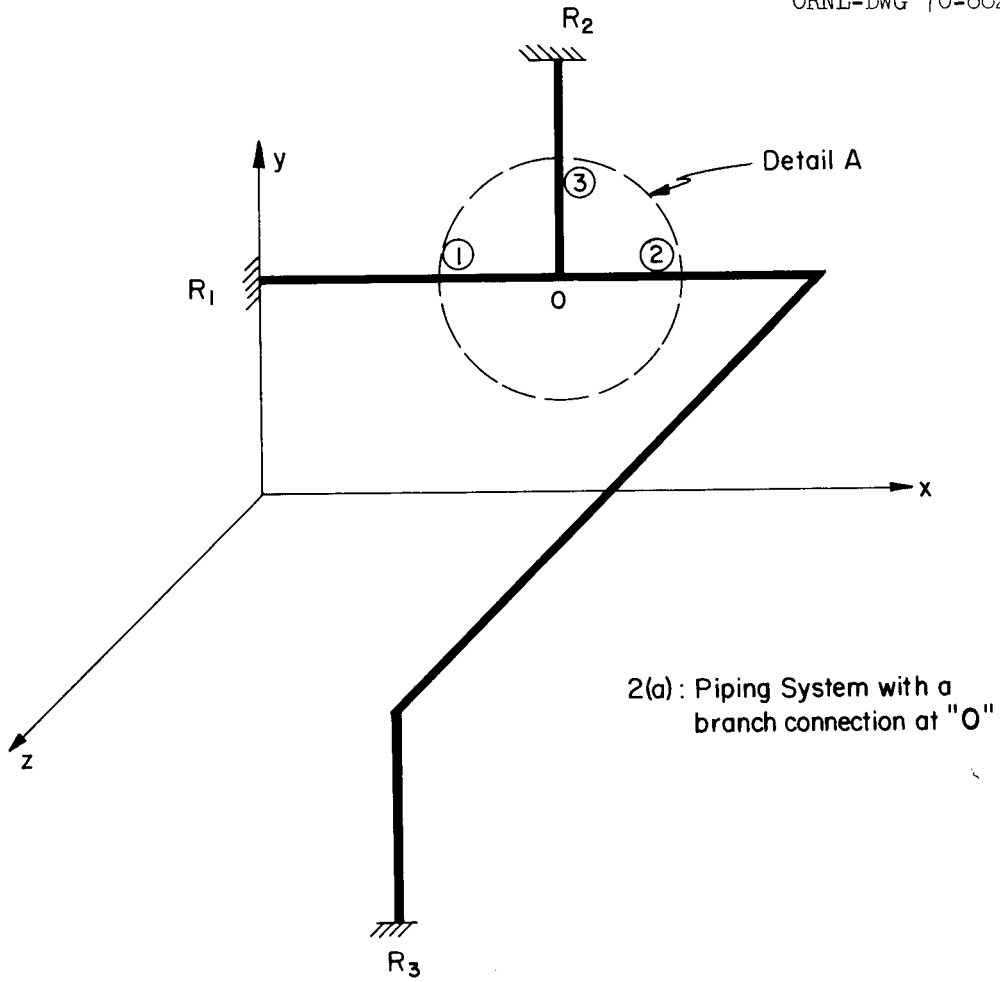
* A letter from R. N. Zogran to the author, December 27, 1968, pointed out this possibility.

LOADINGS AND STRESS INDICES

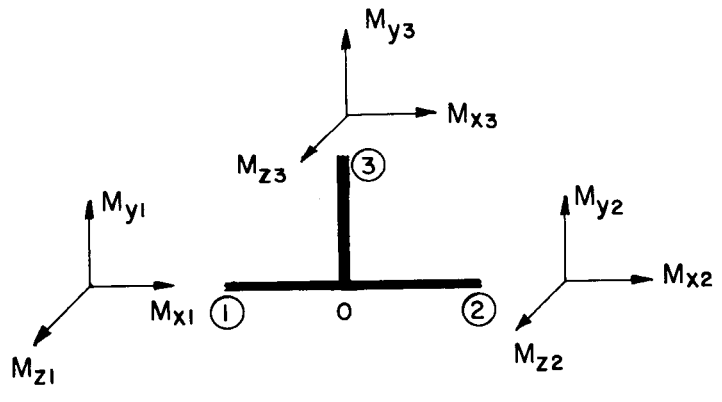
The magnitude of external loadings applied to a branch connection in a piping system is normally determined by a "piping flexibility analysis". Figure 2(a) illustrates a simple piping system containing a branch connection at point "O". As implied by Figure 2(a), a piping flexibility analysis assumes that the piping system, which actually consists of various shell structures, can be modeled as an assemblage of one-dimensional beams. Moments and forces are generated in the piping system by:

- a) Weight or inertia loads of the pipe, piping components (e.g., valves) insulation, contents, etc.
- b) Linear or rotational displacements of restraint points. For example, R_1 of Figure 2(a) may be a pressure vessel nozzle which moves with respect to restraint point R_2 and/or R_3 .
- c) Change in the length of the piping due to change in temperature of the piping.

At a branch intersection point, such as point "O" of Figure 2(a), the piping flexibility analysis will give three orthogonal sets of moments which either are directly, or can be rotated to, the moment sets shown in Figure 2(b). Equilibrium requires that these sets of moments be related by:



2(a): Piping System with a branch connection at "O"



2(b): Detail A , Moments calculated at point "O"

FIGURE 2. PIPING SYSTEM AND SETS OF MOMENTS OBTAINED FROM A PIPING FLEXIBILITY ANALYSIS

$$M_{x1} + M_{x2} + M_{x3} = 0$$

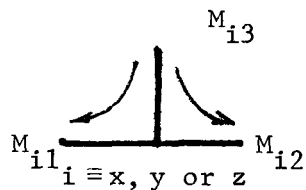
$$M_{y1} + M_{y2} + M_{y3} = 0 \quad (1)$$

$$M_{z1} + M_{z2} + M_{z3} = 0$$

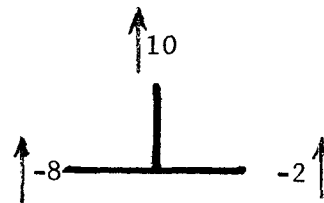
Accordingly, there are only six independent moments at a branch connection. The set of six moments shown in Figure 3 constitute a complete set of moments. This set of moments has been used in experimental and theoretical analyses of branch connections and will be considered herein as the basic set of six independent moment loads. They are identified as M_{ij} , where $i = x, y, z$, $j = r, b$. The set of nine moments from a piping flexibility analysis are similarly identified, except $j = 1, 2, 3$.

In translating data obtained from the basic set of six moments (See Figure 3) for application with the nine moments obtained from a piping flexibility analysis [Figure 2(a)], it is necessary to distinguish that part of the moment that is carried from the branch into one or both ends of the run. There are two general cases.

- 1) Moment through branch is equilibrated by moments at both run ends, with no moment flow through run



, for example



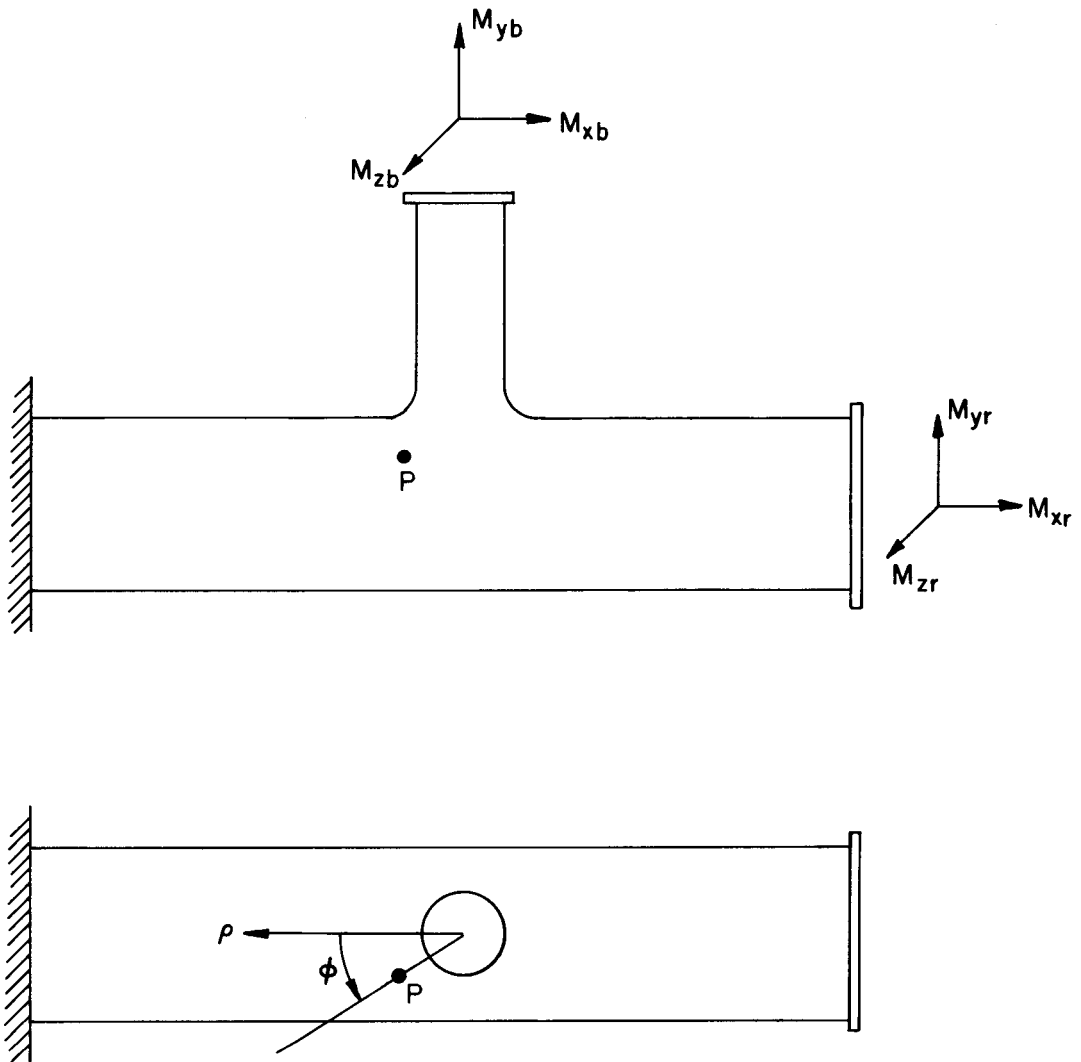
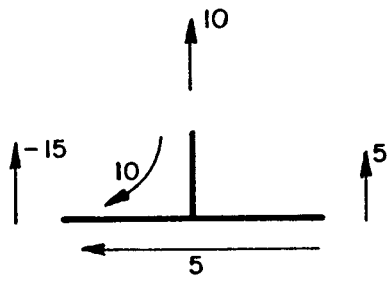
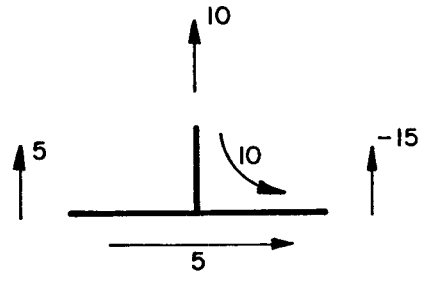


FIGURE 3. EXPERIMENTAL ARRANGEMENTS WITH A COMPLETE SET OF MOMENT LOADINGS

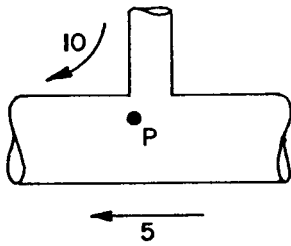
ORNL-DWG 70-6829



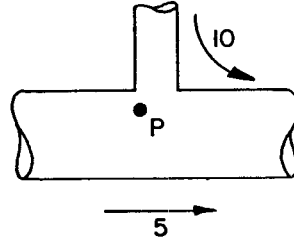
4 (a)



4 (b)



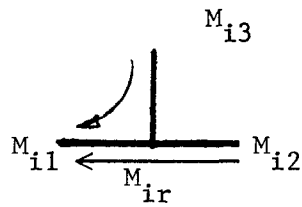
4(c)



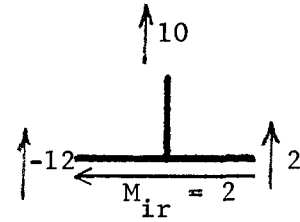
4(d)

FIGURE 4. ILLUSTRATION OF MOMENT FLOW CONCEPT
AT A BRANCH CONNECTION

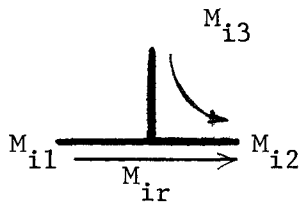
- 2) Moment through branch is equilibrated by moment at one run end with a residual moment flow through the run



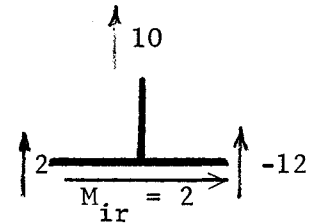
, for example



or



, for example



Relationships between the basic moments and the flexibility analysis moments, appropriate for application with the B31.7 simplified analysis*, are as follows:

$$M_{ir} = 0 \quad \text{for } |M_{i3}| = |M_{i1}| + |M_{i2}| \quad (2)$$

$$M_{ir} = \text{lesser of } |M_{i1}| \text{ or } |M_{i2}|, \text{ for } M_{i3} < |M_{i1}| + |M_{i2}| \quad (3)$$

$$M_{ib} = M_{i3} \quad (4)$$

Perhaps a better way of stating the same relationship is: If the sign of M_{i1} is the same as the sign of M_{i2} , $M_{ir} = 0$; otherwise $M_{ir} = \text{lesser of } M_{i1} \text{ and } M_{i2}$.

* The sign of the moment flow is lost in this formulation; this is a simplification in accordance with the B31.7 (Par 1.705) simplified analysis philosophy that maximum stress intensities due to all loadings occur at the same surface point and are oriented so that they directly add to each other.

Stress Indices

Two types of analyses are covered in B31.7; a "simplified" analysis as covered by 1-705 of B31.7 and a "detailed" analysis as covered by Appendix F of B31.7. While the stress indices derived herein are for the simplified analysis, some discussion of what stress indices would be required for the detailed analysis is pertinent; in part to indicate why such detailed stress indices are not available at this time.

Stress indices for the detailed analysis of branch connections, with moment loadings, might best be given in the form*:

$$\sigma_p = i_p \frac{M_{ij}}{Z} \quad (5)$$

where

σ_p = principal stress at a point, p, on the branch connection
due to moment load, M_{ij}

i_p = principal stress index for M_{ij} at point p

M_{ij} = applied moment

Z = section modulus of pipe (run or branch, as specified by
the stress index nomenclature)

In order to carry out the detailed analysis of B31.7, it would be necessary to have stress indices (i_p) for:

- (1) Each of the six independent moment loads.
- (2) Sufficient surface locations to adequately describe the stress field for each moment (perhaps 50 to 100 locations). These might be expressed as functions of ρ , θ (see Figure 3) and inside, outside or midwall surface.

* Analogous to the i-indices for curved pipe or welding elbows, Table D-309-2 of B31.7.

At each point, a minimum of three quantities would have to be described by the stress index; e.g., the maximum and minimum principal stresses and their orientation with respect to established coordinates.

From the above, it is apparent that a set of detailed stress indices for a given branch connection would consist of 1000 to 2000 quantities. From these quantities, the principal stresses at any point on the branch connection for any combination of moments could be obtained; provided, of course, that superposition is applicable.

Having obtained principal stresses due to moment loads, the next step would be to add the stresses due to internal pressure and thermal gradient stresses, then to determine stress intensities from the principal stresses and complete the analysis by comparing those stress intensities with the allowable stress intensities given in B31.7.

These sets of detailed stress indices could, in principal, be obtained by either a theoretical or experimental stress analysis. Unfortunately, at this time a proven theoretical analysis has not been developed for branch connections with moment loads nor is sufficient test data available to establish detailed stress indices. Even with an available theory and/or test data, the sheer bulk of the detailed stress indices might make their presentation in B31.7 impractical.

There is however, some test data from which a probably conservative estimate of maximum stresses in branch connections can be formulated. This is the approach taken in Table D-201 of B31.7 in which the simplified stress indices (C_2) are given. In principal, we want to establish values of the six C_{2ij} -indices in the equation:

$$\bar{\sigma}_{\max} = C_{2xr} \frac{M_{xr}}{Z} + C_{2yr} \frac{M_{yr}}{Z} \dots\dots\dots C_{2zb} \frac{M_{zb}}{Z} \quad (6)$$

where

$\bar{\sigma}_{\max}$ = maximum stress intensity.

If we consider a test set-up as indicated in Figure 3, with a branch connection thoroughly instrumented with strain gages, the value of C_{2ij} can be established by applying, separately, M_{xr} , M_{yr} M_{zb} . We now choose to define Z for moments applied to the run (M_{xr} , M_{yr} , M_{zr}) as Z_r = section modulus of the run pipe and Z for moments applied to the branch (M_{xb} , M_{yb} , M_{zb}) as Z_b = section modulus of the branch pipe. From the measured maximum stress intensity the value of C_{2ij} is obtained, for example, as:

$$C_{2xr} = \frac{\bar{\sigma}_{xr}}{(M_{xr}/Z_r)} \quad (7)$$

where

C_{2xr} = stress index for M_{xr}

$\bar{\sigma}_{xr}$ = maximum measured stress intensity, as determined from strain gages, under load M_{xr}

M_{xr} = applied moment.

Z_r = section modulus of run pipe.

In developing values for C_{2ij} in the subsequent sections of this report, it will be noted that two kinds of experimental data are used: (1) strain gaged test models and (2) fatigue tests. The fatigue tests, by an evaluation discussed later herein, lead to C_{2ij} factors

which cannot be clearly identified as to whether they represent maximum principal stresses or stress intensities. Maximum principal stresses, σ_{\max} , were used from the strain gage tests. Other than a few known exceptions, the maximum principal stress was also the maximum stress intensity, $\bar{\sigma}_{\max}$. For one test* with torsional moment on the branch (M_{yb}), $\bar{\sigma}_{\max}$ was 1.31 times σ_{\max} ; for other tests** where $\bar{\sigma}_{\max}$ was greater than σ_{\max} , $\bar{\sigma}_{\max}$ was not more than 1.2 times σ_{\max} . The use of maximum principal stresses instead of maximum stress intensity is more than counterbalanced by the assumption inherent in Equations (6) and (7) that maximum stresses due to all of the six moment loads occur at the same location and surface and are oriented so as to directly add to each other.

* Table 3, Reference (8), Model E

** These also occurred for M_{yb} loading.

TEST DATA

Complete sets of test data on branch connections using the test arrangement shown in Figure 3 are quite limited; data known to the author are summarized in Tables 1 and 2. Only one of these test specimens falls within the class of branch connections considered herein; that one being the 12 x 12 x 4 Weldolet connection.

Additional useful test data is shown in Tables 3 and 4. All of this data is for moments (and in a few cases, axial forces) applied to the branch. The references cited do not, in general, indicate where or what kind of reaction forces were applied. In most cases, it appears that run pipe was anchored at both ends. For small d/D branch connections it probably doesn't make much difference where the reaction forces were applied. This assumption is implied in the subsequent analysis of this test data.

Tables 3 and 4 are taken from Reference (14) with some modifications. Table 3 covers "uniform-wall" test models while Table 4 covers test models with some type of local reinforcing around the branch. Some pertinent comments on these tables follow.

- 1) The dimensional nomenclature is that of Figure 1-704.3.3.1 of B31.7; reproduced here as Figure 1 for reference convenience. The additional symbol r_p is used for the effective radius of a pad reinforcing. It is defined as the radius inside which the reinforcement is thicker (measured normal to the cylinder) than $0.5 T_r$.

- 2) Under the "Load" column, M_x , M_y , and M_z correspond to M_{xb} , M_{yb} , and M_{zb} of Figure 3. L indicates an axial force applied to the branch. Sign relationship between positive loads and positive stresses are not maintained in these Tables.
- 3) An entry in the last column (σ'/S) indicates that, in the author's opinion, the maximum reported measured stress was not representative of the actual maximum secondary stress. The values of σ'/S represent extrapolations from three or more strain gages placed along a $\emptyset = \text{constant}$ line up to the discontinuity point. This implies that the strain gage nearest to the discontinuity was a significant distance away from the discontinuity. Where no entry is shown under σ'/S , it is the author's opinion that the maximum reported measured stress is reasonably representative of the actual maximum stress.

Table 5 gives fatigue test data on branch connections with d/D up to 0.63. Reference (11) tests were controlled displacement test analogous to those reported by Markl⁽¹⁵⁾. Reference (12) tests were run with an inertial loading device while Reference (13) tests were run with controlled moment loading. It is significant to note that fatigue failures in all but one test specimen were associated with welds; the one exception being Reference 13, Model D. Crack locations and specimens are described in detail in Reference (14).

Analysis of the data consists of obtaining a stress intensification factor, i_f , by fitting the test data to the equation

$$i_f SN^2 = 245,000 \quad (8)$$

where

i_f = fatigue-based stress intensification factor

S = nominal stress = M/Z_b

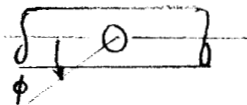
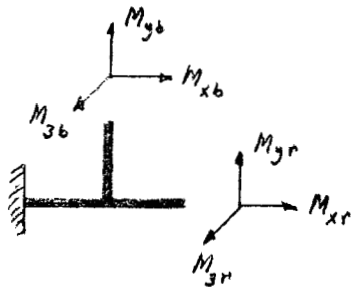
M = moment applied to the branch

Z_b = section modulus of branch pipe

N = cycles-to-failure (through-the-wall crack).

TABLE 1. SUMMARY OF MAXIMUM PRINCIPAL STRESSES FROM STRAIN GAGE TESTS ON FOUR TEES

Load	12 x 12 x 10 XS B16.9 Tees												12-inch SS Pipe Run			
	Steel, M'f'g A				Steel, M'f'g B				Copper-Nickel, M'f'g A				4-inch Weldolet Branch ⁽²⁾			
	Max σ/S	\emptyset	(1)	Gage No.	Max σ/S	\emptyset	(1)	Gage No.	Max σ/S	\emptyset	(1)	Gage No.	Max σ/S	\emptyset	(1)	Gage No.
M_{xr}	5.38	67.5	I	46	4.21	45	I	36	5.36	45.0	I	36	4.29	62.5	0	49
M_{yr}	1.16	-90.0	I	96	1.10	-90	I	96	0.64	90.0	I	58	3.62	90.0	0	513
M_{zr}	1.96	90.0	I	56	1.98	-90	I	96	2.57	90.0	I	56	2.09	-90.0	I	910
M_{xb}	2.46	67.5	0	47	2.58	45	I	38	3.17	90.0	0	55	3.99	90.0	0	59
M_{yb}	3.92	67.5	I	46	3.83	-135	0	85	4.47	45.0	I	36	1.39	45.0	0	33
M_{zb}	1.87	67.5	I	410	2.22	0	0	17	2.08	67.5	I	48	1.32	0	0	13
P	4.29	0	I	110	2.89	0	I	18	2.90	0	I	18	3.08 (2.37)	67.5 180.0	0 I	49 110



σ = maximum principal stress

For Branch: $S = M_{xb}/Z_b; M_{zb}/Z_b; M_{yb}/2Z_b$

For Run: $S = M_{yr}/Z_r; M_{zr}/Z_r; M_{xr}/2Z_r$

$Z_r = 56.7 \text{ in.}^3$ for all four tees (12-inch XS pipe)

$Z_b = 39.4 \text{ in.}^3$ for all tees except Weld 0 Let (10-inch XS pipe)

$Z_b = 3.2 \text{ in.}^3$ for Weld-0-Let (4-inch standard weight pipe)

For pressure loading $S = PD_m/2t = P \times 12.25/(2 \times 0.5) = 12.25 P$ for all four tees.

(1) Surface: I = inside
0 = outside

(2) Dimensional details of the 12 x 12 x 4 Weldolet are shown in Figure 5.

TABLE 2. SUMMARY OF MAXIMUM PRINCIPAL STRESSES FROM STRAIN GAGE TESTS ON A 3 x 3 x 3, Sch 10S, B16.9 TEE AND ON A 10 x 10 x 5, 45°, LATERAL 10.5" O.D. x 0.75" WALL RUN, 5.25 O.D. x 0.375" WALL BRANCH

Load	3" - 10S Tee ⁽¹⁾		10 x 10 x 5, 45° Lateral ⁽⁴⁾		
	Max. σ/S ⁽²⁾	Location ϕ	Max. σ/S ⁽²⁾	Location ϕ	Surface ⁽³⁾
M_{xr}	3.42	60	4.07	210	0
M_{yr}	1.20	60	.94	285	I
M_{zr}	2.45	90	3.19	285	I
M_{xb}	4.24	60	2.40	285	0
M_{yb}	4.19	60	2.11	270	0
M_{zb}	2.14	30	2.97	180	I

--	--

Notes:

(1) Strain gages were placed on outside surface only. Presumably, for some loads, higher stresses existed on the inside surface.

(2) σ = maximum measured principal stress.

For Branch:

$$S = M_{xb}/Z_b; M_{zb}/Z_b; M_{yb}/2Z_b$$

For Run:

$$S = M_{yr}/Z_r, M_{zr}/Z_r, M_{xr}/2Z_r$$

Z_r = section modulus of run pipe

Z_b = section modulus of branch pipe.

(3) I = inside, 0 = Outside

(4) Data from Fung & Lind, "Experimental Stress Analysis of a 45° Lateral Pipe Connection Subjected to External Loadings", U. of Waterloo, Waterloo, Canada, Sept. 1968.

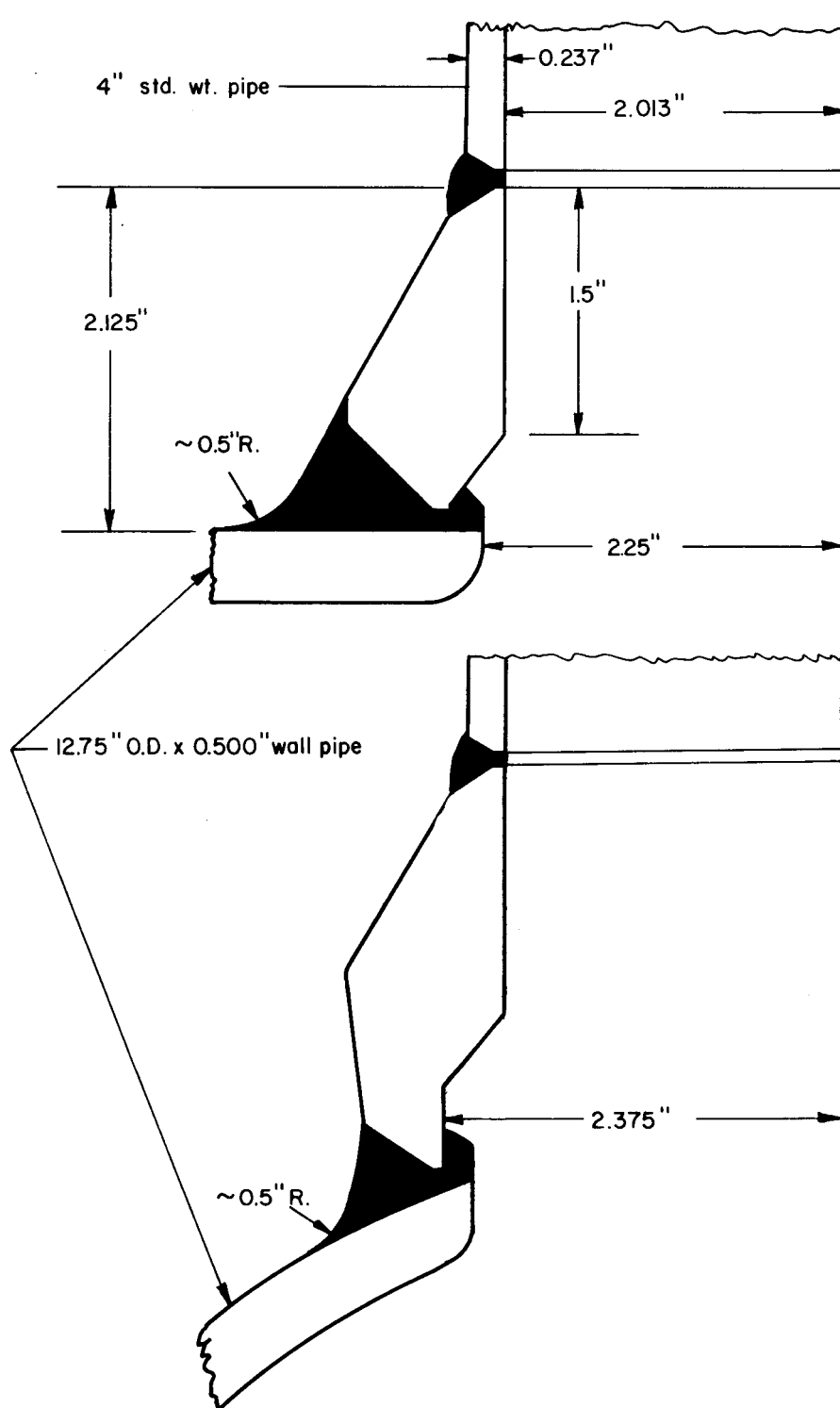


FIGURE 5. DIMENSIONS OF 12 x 12 x 4 WELDOLET BRANCH CONNECTION

TABLE 3. SUMMARY OF TEST DATA FOR EXTERNAL LOADS APPLIED TO
A UNIFORM WALL BRANCH IN A UNIFORM WALL CYLINDER

Ref. No.	Nominal Size ⁽¹⁾	$\frac{R_m}{T_r}$	$\frac{r'_m}{R_m}$	$\frac{T'_b}{T_r}$	$\frac{r'_m}{r_p}$	Load	$\frac{\sigma_{max}}{S}$ (2)	Location & Direction of σ_{max} (3)				$\frac{\sigma'}{S}$ (4)
								Shell	φ	Surface	α	
(3)	56x12 ($T_r=1.3''$)	21.5	.19	.67	.93	M_z	2.49	Run	0	Out	0	4.1(a)
						M_x	4.11	Run	90	Out	0	6.2(a)
						L	7.05	Run	90	Out	0	9.8(a)
	56x12 ($T_r=2.08''$)	13.5	.19	.42	.93	M_z	1.42	Branch	0	Out	90	2.1(a)
						M_x	2.54	Run	45	Out	-	3.8(a)
						L	3.10	Run	45	Out	-	4.6(a)
(4)	24x4	38	.18	.76	.95	M_z	3.75	Run	0	Out ^(b)	0	4.5
						M_x	7.18	Run	90		0	10.
	24x12	38	.53	.80	.98	M_z	2.43	Run	30		130	5.1
						M_x	6.22	Run	90		0	12.
	24x24	38	1.00	1.00	.99	M_z	5.15	Branch	90		45	8.4
						M_x	11.2	Branch	90		90	14.
(5)	36x4 (E)	46.5	.12	.42	.96	M_z	1.4	Run ^(c)	0 ^(d)	Out	0	2.1(a)
						M_x	2.7		90	Out	0	3.5
						L	6.0		90	Out	0	8.1
	36x6 (C)	46.5	.18	.75	.96	M_z	4.25		0	Out	0	4.7
						M_x	8.5		90	Out	0	10.5
						L	14.0		90	Out	0	16.7
(6)	10x10	8	1.00	1.00	.94	M_z	2.2	Branch	45	Out	-	? (e)
						M_x	3.4	Branch	67.5	Out	-	? (e)
(7)	48x6	39	.13	.45	.96	M_z	3.0	Branch	0	Out	0	3.1(a)
						M_x	4.4	Branch	90	Out	90	4.4(a)
						L	9.3	Branch	90	Out	90	9.9(a)
(8)	20x6 ^(f) (L)	9.5	.32	.43	.93	M_z	1.73	Trans.	0	Out	90	-
						M_x	2.19	Trans.	90	Out	90	-

TABLE 3. (Continued)

Ref. No.	Nominal Size ⁽¹⁾	$\frac{R_m}{T_r}$	$\frac{r'_m}{R_m}$	$\frac{T'_b}{T_r}$	$\frac{r'_m}{r_p}$	Load	$\frac{\sigma_{max}}{S}$ (2)	Location & Direction of σ_{max} (3)				$\frac{\sigma'}{S}$ (4)
								Shell	φ	Surface	α	
(8)	20x12 ^(f) (D)	9.5	.63	.69	.95	M _Z	2.70	Trans.	30	Out	168	-
						M _Z	4.36	Trans.	90	Out	90	-
						L ^x	8.70	Branch	90	In	90	-
						M _y	1.59	Trans.	60	In	31	-
	20x12 ^(f) (E)	9.5	.65	.38	.97	M _Z	2.03	Branch	15	Out	172	-
						M _Z	2.33	Branch	75	Out	175	-
						L ^x	5.25	Branch	75	Out	24	-
						M _y	1.71	Trans.	0	Out	42	-
	20x12 ^(f) (R)	9.5	.63	.69	.95	M _Z	3.53	Fillet	0	Out	90	-
						M _Z	8.55	Branch	90	Out	90	-
						L ^x	12.5	Branch	90	Out	90	-
	20x20 (S)	9.5	1.00	1.00	.95	M _Z	5.2	Fillet	0	Out	90	-
M _Z						5.25	Run	60	Out	24	-	
L ^x						23.6	Run	45	Out	46	-	
(9)	24x12 (C-1)	115	.50	1.00	.99	M _Z	18.5	Fillet	60	Out	0	-
						M _Z	90.	Fillet	90	Out	0	-
						L ^x	100.	Fillet	82.5	Out	0	-

(1) Symbols in parentheses under the nominal size give further identification of the test models in accordance with the references cited.

(2) S = nominal stress in nozzle

$$S = \frac{M_z \text{ or } M_x}{Z_b} = \frac{M}{\pi(r'_m)^2 T'_b}$$

$$S = \frac{M_y}{Z_b}$$

Axial Force

$$S = \frac{L}{A} \\ A = 2\pi r'_m T'_b$$

σ_{max} = maximum measured stress

TABLE 3. (Continued)

Footnotes to Table 3

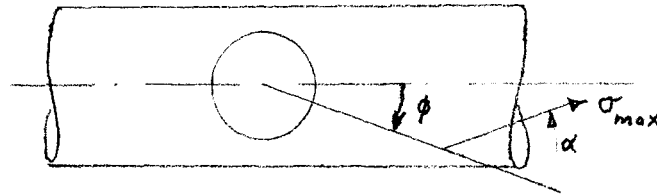
(3) Location and Direction of Maximum Measured Stress

Column Shell identifies whether σ_{\max} occurred on branch, run or the juncture between run and branch. For Reference (8) models L, D, and E (drawn-outlet tees), trans. means σ_{\max} occurred in the radius between cylinder and nozzle. For References (8) and (9) fillet means σ_{\max} occurred in the (ground-off) fillet weld between cylinder and nozzle.

Column φ identifies location around nozzle.

Column Surface, Out means σ_{\max} occurred on outside surface; In means σ_{\max} occurred on the inside surface.

Column α identifies direction of σ_{\max} as shown in sketch.



- (4) σ'/S is an approximate extrapolated value of test data to the toe of the fillet weld between cylinder and nozzle. It does not include stress concentrations at the toe of the fillet weld.
- (a) Extrapolated stress in cylinder. Test data is not sufficient to estimate maximum stress in branch pipe; in some models, the maximum stress in the nozzle is probably higher than the stress shown.
- (b) Strain gages on the outside only.
- (c) No data for stresses in nozzle.
- (d) Test data at $\varphi = 0$ and $\varphi = 90$ only.
- (e) Data insufficient to extrapolate to maximum stress on either cylinder or nozzle.
- (f) These test models are "drawn-outlet" tees.

TABLE 4. SUMMARY OF TEST DATA FOR EXTERNAL LOADS APPLIED TO BRANCH, MODELS WITH LOCAL REINFORCING

Ref. No.	Nominal Size ⁽¹⁾	$\frac{R_m}{T_r}$	$\frac{r'_m}{R_m}$	$\frac{T_{b'}}{T_r}$	$\frac{r'_m}{r_p}$	Load	$\frac{\sigma_{max}}{S}$ (2)	Location & Direction of σ_{max} (3)				$\frac{\sigma'}{S}$ (4)
								Shell	φ	Surface	α	
10	24x4 ^(a) (Saddle)	38	.18	.76	.44	M_x	2.6	Run	90°	Out	0	4. (g)
	24x8 ^(a) (Saddle)	38	.35	.80	.48	M_x	4.8	Run	90°	Out	0	7. (g)
	24x12 ^(a) (Saddle)	38	.53	.80	.53	M_x	4.9	Run	90°	Out	0	7. (g)
	24x4 ^(b) (Pad)	38	.18	.76	.55	M_x	3.3	Run	90°	Out	0	5. (g)
	24x8 ^(b) (Pad)	38	.35	.80	.53	M_x	3.7	Run	90°	Out	0	6. (g)
	24x12 ^(b) (Pad)	38	.53	.80	.51	M_x	5.7	Run	90°	Out	0	8. (g)
(6)	10x10 ^(c) (Pad)	8	1.00	1.00	.94	M_z M_x	1.7 2.0	Branch Branch	22.5 61.5	Out Out	- -	? (h) ? (h)
	8x8 ^(d) (Tee)	8	1.00	1.00	.94	M_z	1.4 ⁽ⁱ⁾	Run	~80	In	-	-
	48x6 ^(e) (Pad)	39	.13	.45	.60	M_z M_x L^x	1.2 4.3 8.5	Branch Branch Branch	0 90 90	Out Out Out	0 0 90	1.4 (g) 4.3 (g) 8.4 (g)
(8)	20x6 ^(f) (F)	9.5	.32	.43	.50	M_z M_x L^x	1.41 1.49 3.28	Branch Branch Juncture	22.5 67.5 45	Out Out Out	0 2 9	- - -
	20x6 ^(f) (I)	9.5	.32	.43	.54	M_z M_x	1.15 1.14	Branch Juncture	22.5 90	Out Out	5 90	- -
	20x6 ^(f) (J)	9.5	.32	.43	.73	M_z M_x	1.42 1.18	Branch Branch	22.5 67.5	Out Out	7 4	- -

FOOTNOTES FOR TABLE 4.

(1) Symbols in parentheses under the nominal size give further identification of the test models in accordance with the references cited.

(a) Saddle Dimensions:	24x4	24x8	24x12
T_s	0.375"	0.468"	0.468"
D_s	9.625"	17.25"	23.75"
H_s	2.0"	3.0"	3.5"

T_s = Saddle thickness (average), D_s = saddle outside diameter, H_s = height of saddle above cylinder surface.

(b) Pad Dimensions:	24x4	24x8	24x12
T_p	0.375"	0.375"	0.375"
D_p	7.75"	15.75"	24.5"

T_p = pad thickness, D_p = pad outside diameter.

(c) Pad Dimensions: $T_p = 0.625"$, $D_p = 19.875"$.

(d) This specimen is described as an 8" Sch.80 welding tee. Presumably, it met the dimensional and strength requirement of ASA B16.9 and was typical of tees sold under this standard.

(e) Pad Dimensions: $T_p = 0.625"$, $D_p = 10.5"$

(f) Dimensions of these specimens are shown in Figure 6.

(2) S = nominal stress in nozzle	M_z or M_x $S = M/Z$ $Z = \pi (r'_m)^2 T'_b$	M_y $S = M_y/yZ$	L $S = L/A$ $A = 2\pi r'_m T'_b$	σ_{max} = maximum measured stress
-------------------------------------	--	-----------------------	--	--

(3) Location and Direction of maximum measured stress

Column Shell identifies whether σ_{max} occurred on nozzle, cylinder or the juncture between cylinder and nozzle. For Reference (8), models F, I, & J. juncture means σ_{max} occurred in the radius between cylinder and nozzle.

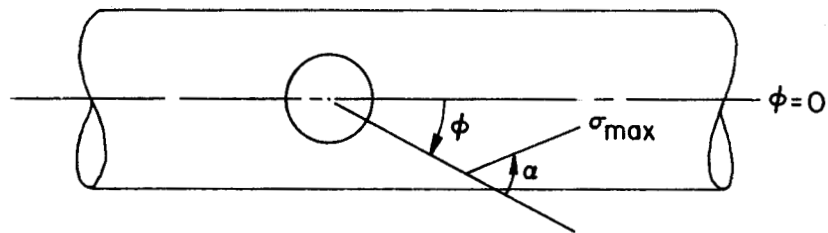
Column ϕ identifies location around nozzle; see sketch on next page.

Column Surface, Out means σ_{max} occurred on outside surface; In means σ_{max} occurred on the inside surface.

Footnotes for Table 4. (Continued)

(3) (Continued)

Column α identifies direction of σ_{\max} as shown in sketch

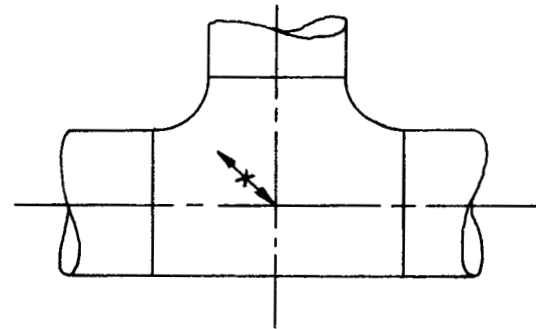


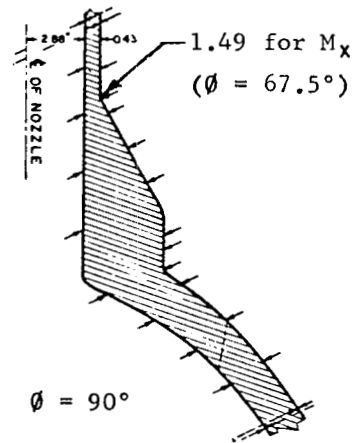
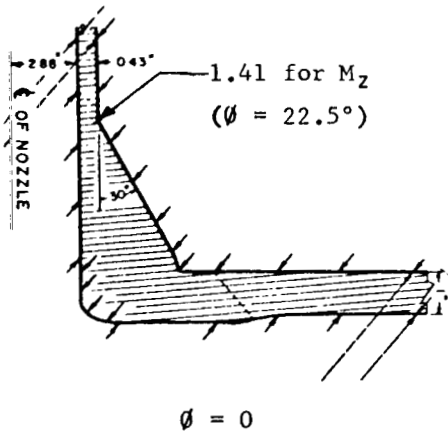
(4) σ'/S is an extrapolated value of test data to the toe of the fillet weld between cylinder and pad or saddle. It does not include stress concentrations at the toe of the fillet weld.

(g) Extrapolated stress in cylinder. Test data is not sufficient to estimate maximum stress in nozzle; in some models, the maximum stress in the nozzle is probably higher than the stress shown.

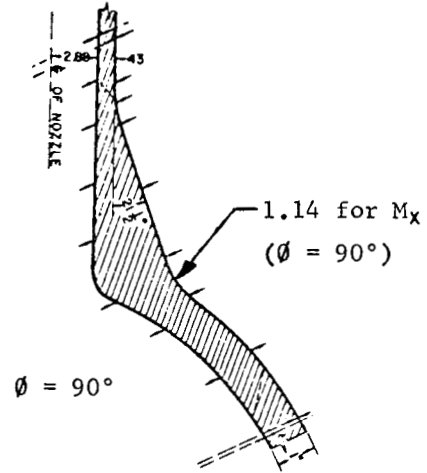
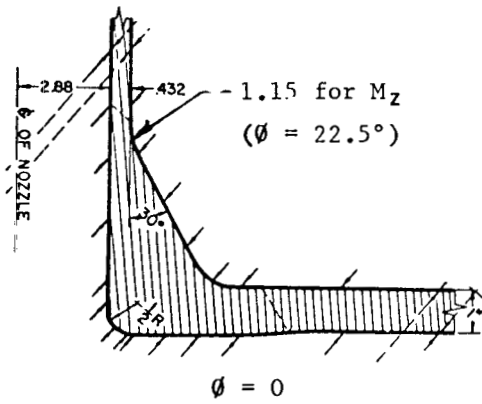
(h) Data insufficient to extrapolate to maximum stress in either cylinder or nozzle.

(i) Location and direction of σ_{\max}/S shown in sketch at right.

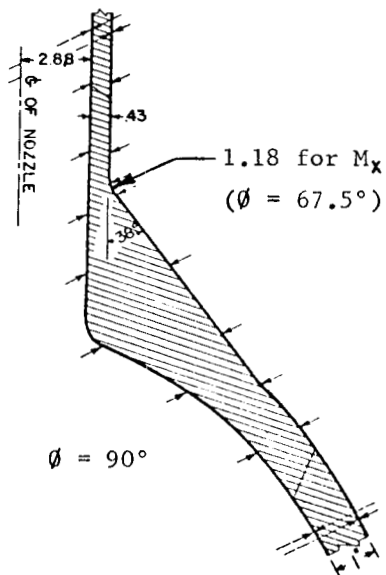
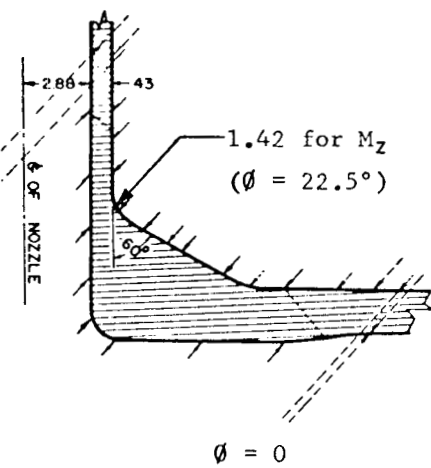




MODEL F



MODEL I



MODEL J

FIGURE 6 . CONTOURS OF MODELS F, I, AND J, REFERENCE (8) AND MAGNITUDES AND LOCATIONS OF MAXIMUM STRESS INDICES

TABLE 5. SUMMARY OF RESULTS OF FATIGUE TESTS OF TEES,
DATA FOR $r'_m/R_m < 1.00$

Ref. No.	Nominal Size	Reinforcing (1)	$\frac{R_m}{T_r}$	$\frac{r'_m}{R_m}$	$\frac{T'_b}{T_r}$	$\frac{r'_m}{r_p}$	Load	No. of Specimens	i_f , ⁽²⁾ Test Data
(11)	12x4	Saddle ^(a)	34.	.34	.89	.57	M_z M_x	4	1.19
								2	4.18
(12)	16x6	Pad ^(b)	15.5	.41	.56	.52	M_z M_x	13 ^(f)	3.6
								4	2.8
	16x6	Saddle ^(c)	15.5	.41	.56	.55	M_z M_x	13	2.4
								3	2.8
	16x6	None ^(d)	15.5	.41	.56	.96	M_z	7	4.4
16x6	None ^(d)	7.5	.42	.28	.96	M_z	7	2.4	
(13)	20x6 (L)	None ^(d)	9.5	.32	.43	.93	M_x	1	1.2
	20x12 (D)	None ^(d)	9.5	.63	.69	.95	M_x	1	2.5
	20x12 (R)	None	9.5	.63	.69	.95	M_x	1	3.9

- (1) (a) Saddle dimensions: 0.368" thick x 7.3125" O.D. x 1.25" height above cylinder surface.
 (b) Pad dimensions: 0.500" thick x 12.125" O.D.
 (c) Saddle dimensions: 0.500" thick x 11.625" O.D. x 1.5" height above cylinder surface.
 (d) Drawn outlet tee.

(2) Value of i_f in Equation; $i_f^{SN} = 245,000$.

(f) Part of the fatigue tests were run with 800 psi static internal pressure (nominal pressure stress of 12,500 psi for D/T = 31; 6000 for D/T = 15. No significant difference in fatigue life was observed between those specimens with pressure and those without pressure.

PROPOSED INDICES FOR B31.7Moment Loading Through Branch

Inspection of the test data shown in Tables 1 through 5 indicate that, in most available comparisons, an out-of-plane moment (M_x) produces higher stresses than an in-plane moment (M_z). Unfortunately, there are some exceptions and available data is not consistent enough to take advantage of this trend. Instead, we seek a general formulation for C_{2b} so that it is in accord with test data for the moment producing the highest stress; generally, this is M_x . A formulation which fits the test data of Tables 1 through 4 is:

$$C_{2b} = 3.0 (R_m/T_r)^{2/3} (r'_m/R_m)^{1/2} (T'_b/T_r)(r'_m/r_p) \quad (9)$$

Equation (9) is compared with Bijlaard-Wichman⁽¹⁶⁾ analysis in Table 6. This analysis is based on Bijlaard's⁽¹⁷⁾ work using shell-theory for a distributed load on the surface of a cylinder and empirical modification thereof by Wichman, et. al. Equation (9) is compared, in particular, with the analysis for an out-of-plane (circumferential) moment, M_c , and the circumferential stress, σ_ϕ , due to the circumferential moment; this moment-stress combination is usually the highest obtained from the analysis. As can be seen in Table 6, Equation (9) gives about the same results as the Bijlaard-Wichman analysis for $r'_m/R_m = 0.5$ and is conservative with respect to the Bijlaard-Wichman analysis for small r'_m/R_m . Equation (9) is compared with measured stresses in Table 7. Equation (9) is conservative with

TABLE 6. COMPARISON OF EQUATION (9) FOR C_{2b} WITH BIJLAARD-WICHMAN. CALCULATED σ_{ϕ} -STRESSES FOR M_x ON BRANCH

$\frac{r'_m}{R_m}$	$\frac{R_m}{T_r}$	CBW(1) $(T'_b/T_r)(r'_m/r_p)$	C_{2b} (2) $(T'_b/T_r)(r'_m/r_p)$
.5	5	5.29	6.203
	15	12.8	12.90
	50	33.9	28.79
.4	5	4.35	5.548
	15	11.1	11.54
	50	27.9	25.75
.3	5	3.38	4.805
	15	8.95	9.994
	50	22.0	22.30
.15	5	1.72	3.397
	15	5.07	7.067
	50	14.8	15.77
.05	5	.59	1.961
	15	1.71	4.080
	50	5.80	9.104

$$(1) \quad CBW = \frac{\sigma_{\phi}}{M_c/\pi r^2 t} = \left[\frac{N_{\phi}}{M_c/R^2\beta} \right] \frac{\pi r^2 t}{R^2\beta T} + \left[\frac{M_{\phi}}{M_c/R\beta} \right] \frac{6\pi r^2 t}{R\beta T^2}$$

$\beta = 0.875 r_p/R$; $r = r'_m$, $R = R_m$, $t = T'_b$, $T = T_r$, Figure 1.

$$CBW = \left\{ \left[\frac{N_{\phi}}{M_c/R^2\beta} \right] \times 3.60 + \left[\frac{M_{\phi}}{M_c/R\beta} \right] \times 21.6 \frac{R}{T} \right\} \frac{r}{R} \frac{t}{T} \frac{r}{r_p}$$

Values of $[N_{\phi}/(M_c/R^2\beta)]$ and $[M_{\phi}/(M_c/R\beta)]$ obtained from Reference (16), Figures 1A and 3A. Values do not include the stress concentration factors given in Reference (16).

(2) Equation (9).

TABLE 7. COMPARISON OF EQUATION (9) FOR C_{2b} WITH MEASURED ELASTIC STRESSES, d/D UP TO 0.65

Test Data Table No.	Ref. No.	Test Model Identification	$\frac{R_m}{T_r}$	$\frac{r'_m}{R_m}$	$\frac{T'_b}{T_r}$	$\frac{r'_m}{r_p}$	C_{2b} Eq (9)	Test Data $\sigma_{max} / [M/\pi(x'_m)^2 T'_b]$			Bijlaard-Wichman, CBW(1)
								M_{xb}	M_{yb}	M_{zb}	
1	--	Weldolet	12.25	.35	.47	.73	3.28	3.99	1.39	1.32	2.8
2	3	56 x 12(1.3)	21.5	.19	.67	.93	6.30	6.2	--	4.1	5.2
	3	56 x 12(2.08)	13.5	.19	.42	.93	2.90	3.8	--	2.1	2.2
	4	24 x 4	38.0	.18	.76	.95	10.39	10.	--	4.5	9.7
	4	24 x 12	38.0	.53	.80	.98	19.35	12.	--	5.1	23.5
	5	36 x 4	46.5	.12	.42	.96	5.42	3.5	--	2.1	4.9
	5	36 x 6	46.5	.18	.75	.96	11.85	10.5	--	4.7	11.3
	7	48 x 6	39.0	.13	.45	.96	5.37	4.4	--	3.1	4.7
	8	20 x 6(L)	9.5	.32	.43	.93	3.04	2.19	--	1.73	2.5
	8	20 x 12(D)	9.5	.63	.69	.95	7.00	4.36	1.59	2.70	7.3
	8	20 x 12(E)	9.5	.65	.38	.97	4.00	2.33	1.71	2.03	4.2
	8	20 x 12(R)	9.5	.63	.69	.95	7.00	8.55	--	3.53	7.3
	9	24 x 12	115.0	.50	1.00	.99	49.67	90.	--	18.5	65.
	4	10	24 x 4, Saddle	38.	.18	.76	.44	4.81	4.	--	--
10		24 x 8, Saddle	38.	.35	.80	.48	7.70	7.	--	--	*
10		24 x 12, Saddle	38.	.53	.80	.53	10.47	7.	--	--	*
10		24 x 4, Pad	38.	.18	.76	.55	6.01	5.	--	--	4.5
10		24 x 8, Pad	38.	.35	.80	.53	8.51	6.	--	--	7.7
10		24 x 12, Pad	38.	.53	.80	.51	10.07	8.	--	--	*
7		48 x 6, Pad	39.	.13	.45	.60	3.36	4.3	--	1.4	2.5
13		20 x 6(F)	9.5	.32	.43	.50	1.64	1.49	--	1.41	1.2
13		20 x 6(I)	9.5	.32	.43	.54	1.77	1.14	--	1.15	1.3
13		20 x 6(J)	9.5	.32	.43	.73	2.39	1.18	--	1.42	1.9

(1) CBW is calculated from data given in Reference (16) as shown by footnote (1) to Table 6. An asterisk in this column indicates that β is above range of the graphs. These values do not include the stress concentration factors given in Reference (16).

respect to maximum measured stresses in almost all comparisons. Stresses obtained from the Bijlaard-Wichman analysis are also shown in Table 7.

Comparisons of Equation (9) with fatigue test data are shown in Table 8. The stress intensification factors shown in Table 5 are related to the stress intensification of a typical girth butt weld taken as unity. Because the typical girth butt weld itself has a stress intensification factor of around 2 as compared to a polished bar, an appropriate comparison is between Equation (9) and two times the factors shown in Table 5. Examination of Table 8 shows that Equation (9) is not conservative as compared with the test results of Reference (12). However, these fatigue failures were associated with welds. In particular, the failures in the heavy wall drawn outlet test models occurred at a girth butt weld as shown in Figure 7. A significant peak stress would be expected to occur at such a weld.

The proceeding discussion brings up several pertinent questions:

- (1) Is the stress represented by Equation (9) properly classified as a "secondary stress" within the intent of B31.7?
- (2) Is there a need for a "peak" stress index for the designs covered by Fig. 1-704.3.3.1 of B31.7 (Figure 1 herein)?
- (3) Is Equation (9) adequate to cover all possible configurations covered by Fig. 1-704.3.3.1 of B31.7?

The authors comments on these questions are given below.

(1) Equation (9), in the sense that it is an approximation of a shell analysis, is representative of a secondary stress, i.e., a stress consisting of a membrane portion and a linear bending portion. It could be contended that the stresses are highly localized and hence could be

TABLE 8. COMPARISON OF EQUATION (9) FOR C_{2b} WITH FATIGUE TEST DATA OF TABLE 5

Ref. No.	Test Model Identification	$\frac{R_m}{T_r}$	$\frac{r'_m}{R_m}$	$\frac{T'_b}{T_r}$	$\frac{r'_m}{r_p}$	C_{2b} Eq. (9)	Test Data, $2xi_f$		CBW (1)
							M_{xb}	M_{zb}	
(11)	12 x 4, Saddle	34.	.34	.89	.57	9.31	8.36	3.38	8.5
(12)	16 x 6, Pad	15.5	.41	.56	.52	3.48	5.6	7.2	*
	16 x 6, Saddle	15.5	.41	.56	.55	3.68	5.6	4.8	*
	16 x 6, D.O.	15.5	.41	.56	.96	6.42	--	8.8	6.2
	16 x 6, D.O.	7.5	.42	.28	.96	2.00	--	4.8	1.7
(13)	20 x 6, L	9.5	.32	.43	.93	3.04	2.4	--	2.5
	20 x 12, D	9.5	.63	.69	.95	7.00	5.0	--	7.3
	20 x 12, R	9.5	.63	.69	.95	7.00	7.8	--	7.3

(1) CBW is calculated from data given in Reference (16) as shown by footnote (1) of Table 6. An asterisk in this column indicates that β is above range of the graphs. These values do not include the stress concentration factors given in Reference (16).

ORNL-DWG 70-6832

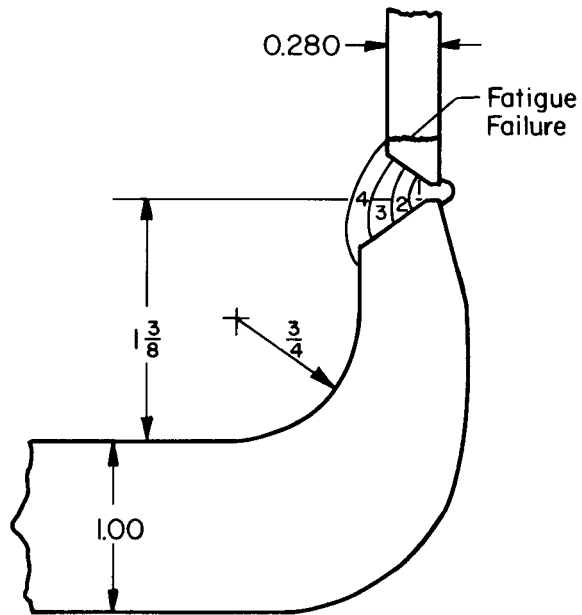


FIGURE 7. WELD CONFIGURATION AND LOCATION OF FATIGUE FAILURES, REFERENCE (12) TESTS ON 16 x 6 DRAWN OUTLET BRANCH CONNECTION WITH $R_m/T_r = 7.5$

at least partially classified as peak stresses. However, the author's recommendation is that, for the present, stresses given by Equation (9) be considered as secondary stresses.

(2) A peak stress in excess of that indicated by Equation (9) could exist if the transition radius r_2 of Figure 1 were small. At present, B31.7 does not give any limits* on the radius r_2 . If this radius is specified as:

$$r_2 = \text{larger of } T_r/2 \text{ or } T_b/2 \quad ,$$

then, in the author's opinion, a K_2 -index of 1.0 is adequate.

(3) It should be noted that, for small branch connections with $R_m/T_r = \sim 10$, Equation (9) may give a value of C_{2b} less than one. For example, consider a 2" branch in a 24" pipe constructed as shown in Figure 1(c). Assume that $R_m/T_r = 10$, $r'_m/R_m = 0.1$, $r'_m/r_p = 0.667$. Also, as a limiting case, consider that both branch pipe and run pipe wall thicknesses are those necessary for the pressure loading, in which case $T'_b/T_r \approx r'_m/R_m$. Equation (9) then gives

$$C_{2b} = 3.0 (10)^{2/3} (0.1)^{1/2} (0.1)(0.667) = 0.29 \quad .$$

Obviously, this value of C_{2b} does not represent the maximum secondary stress in the branch connection because the branch pipe itself has a stress index of at least one. Equation (9), to the extent that it has a theoretical basis, represents the stress in the run pipe at the juncture with the nozzle or local reinforcing. The C_{2b} -value of 0.29 is presumably representative of the stress at this juncture. However, higher stresses may occur at the

* Except in D-313.1.

branch pipe-to-pad juncture as shown in Figure 6. Accordingly, some lower bound on C_{2b} is necessary for those configurations where the maximum stress occurs at the juncture of the reinforcing with the branch pipe. It is suggested that a lower bound on C_{2b} of 1.5 is adequate, provided that the value of r_3 in Figure 1 is limited as follows.

The radius r_3 is not less than the greater of the following:

- (1) $0.002 \theta d_o$, where θ (degrees) and d_o are as defined in Figure 1.
- (2) $2 (\sin \theta)^3$ times offset for the configurations shown in Figure 1(a) and 1(b).

If there is a girth butt weld at the juncture of reinforcing to the branch pipe, an appropriate K_2 -factor should be used; 1.8 for "as welded" or 1.1 for "flush" welds. (See Table D-201 of B31.7 for definitions of these.)

Moment Loading Through Run

Test data on this loading condition are very scarce; the only applicable data known to the writer are that shown in Table 1 for the 12 x 4 Weldolet branch connection. Bijlaard's analysis, of course, is not applicable. For small holes in cylinders, some bounds on stress can be established, i.e.:

For a small hole in a cylinder, located 90° from the plane of the applied moment M_{yr} or M_{zr} :

$$\sigma_{\max} = 3 \frac{M}{Z_r} \quad (10)$$

For a small hole in a cylinder with applied moment M_{xr} (torsion)

$$\sigma_{\max} = 4 \frac{M_{xr}}{2Z_r} = 2 \frac{M_{xr}}{Z_r} \quad (11)$$

Comparison of the test data given in Tables 1 and 2 with Equations (10) and (11) indicates some qualitative agreement. For example, for M_{xr} (torsion), the test data give maximum stresses of from 3.42 to 5.38 times $M_{xr}/2Z_r$. For M_{zr} (axis of the opening 90° to the plane of the moment), the test data give maximum stresses of from 1.96 to 3.19 times M_{zr}/Z_r . For M_{yr} (axis of the opening in the plane of the moment), the test data give maximum stresses of from 0.62 to 1.20 times M_{yr}/Z_r . For M_{yr} , the small-opening approximation would indicate zero stress. Of course, the test models were not "small openings". For the Weldolet model, that the maximum reported index is less than unity simply reflects that strain gages were not extended all the way to the side of the run. One significant part of the detailed results is the following. A row of gages were placed along the $\theta = 90^\circ$ as shown in Figure 8. For M_{yr} , the results were:

Gage No.	$\frac{\sigma}{S}$
51	< 0.1
52	< 0.1
53	< 0.1
54	< 0.1
55	< 0.1
56	< 0.1
57	< 0.1
58	< 0.1
59	.32
510	< 0.1
511	.50
512	.23
513	.62 (max)
514	.42
516	.58

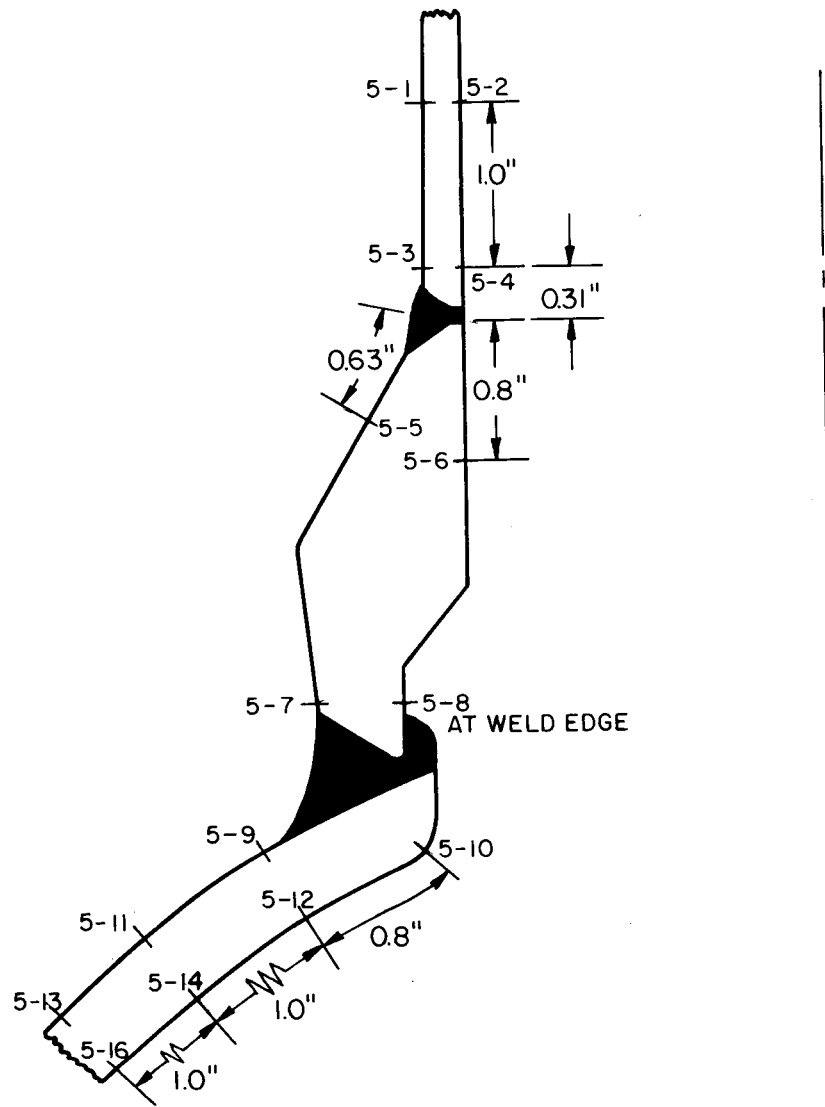


FIGURE 8. STRAIN GAGE LOCATIONS AT $\theta = 90^\circ$,
12 x 12 x 4 WELDOLET

These results are unusual but reasonable in that they indicate that stresses are lower in the vicinity of the branch connection than they are away from the connection. Gages 513 and 516 are located about 50° from the side where the nominal stress index is about 0.65, a value in reasonable agreement with the test results.

With this admittedly small amount of background, we now seek a general formulation for use in the B31.7 simplified analysis. As for loading through the branch, we want to select a stress index which is conservative for that moment which gives the highest stress, presumably either M_{xr} or M_{zr} . The proposed formulation for C_{2r} and K_{2r} is:

$$C_{2r} = 0.8 (R_m/T_r)^{2/3} (r'_m/R_m) \quad (12)$$

but not less than 1.0

$$K_{2r} = 2.0$$

The product $C_{2r}K_{2r}$ shall be a minimum of 3.0.

Table 9 gives C_{2r} factors over the range of applicability.

First, it will be noted that stress due to moments through the run are divided into secondary stresses and peak stresses. The concept here is that for small branch connections, even with local stresses well above twice the yield strength, there cannot be any continued plastic deformation because the bulk of the run pipe will control the deformations at the small branch connection.

The $(R_m/T_r)^{2/3}$ factor is used in Equation (12) for consistency with the factor used for B16.9 tees and the author's intuition that this kind of parameter is significant. One notes that Equation (12) gives

TABLE 9. COMPARISON OF PRESENT C_2 -INDICES AND PROPOSED C_{2r} -INDICES FOR "BRANCH CONNECTIONS PER SUBDIV. 1-704.3", FOR RUN PIPE

$\frac{R_m}{T_r}$	Present C_2 (1)	Proposed C_{2r} for r'_m/R_m of: (2)				
		0.1	0.2	0.3	0.4	0.5
5	2.37	.23*	.47*	.70*	.94*	1.17
10	3.77	.37*	.74*	1.11	1.49	1.86
15	4.94	.49*	.97*	1.46	1.95	2.43
30	7.84	.77*	1.54	2.32	3.09	3.86
50	11.02	1.09	2.17	3.26	4.34	5.43

$$(1) C_2 = 1.8/(3.3T/R)^{2/3}$$

$$(2) C_{2r} = 0.8(R_m/T_r)^{2/3} (r'_m/R_m); \text{ Equation (12)}$$

* Controlled by "not less than 1.0"

a conservative result as compared with the one test model, i.e.,

$$C_{2r}K_{2r} = 1.6 \left(\frac{6.125}{0.5} \right)^{2/3} \left(\frac{4.26}{12.25} \right) = 2.96 .$$

The test data (Weldolet, Table 1) gives stress indices of 2.15 for M_x/Z_r , 0.62 for M_y/Z_r , and 2.09 for M_z/Z_r .

Resultant Moment

Equations (9) through (12) of B31.7 introduce the moment load by the use of the resultant moment, M_i . This permits a concise presentation of the equations but may impose a limitation on refinements of the simplified analysis. It should be noted that the piping system analysis gives one (or three, for branch connection points) orthogonal sets of moments of each point. If stress indices were available for each moment direction (as they are for elbows or curved pipe), then each moment could be multiplied by its appropriate stress index, thus eliminating some of the conservatism introduced by using the highest stress index for each moment.

The simplified analysis, as applied to branch connections, is conservative because (1) it is assumed that maximum stresses due to the various loads all occur at the same point on the component and are aligned so as to add to each other, and (2) for moment loadings, the highest stress index for moments on the branch is used for all three moments on the branch and similarly for moments on the run. Some balance to this conservatism is applied because:

- (1) The stress indices for moment loadings are actually representative of maximum principal stresses--not stress intensities. However, in most tests the maximum* principal stress was also the maximum stress intensity, i.e., the principal stresses at the point were of the same sign and elsewhere on the component the principal stress differences were smaller than the maximum* principal stress.
- (2) If two orthogonal moments, M_i and M_j , actually produced identical stress intensities at the same point on a component, then the stress at that point would be $C_2 M_i/Z + C_2 M_j/Z$. However, use of the resultant moment would give a stress of $C_2 \sqrt{M_i^2 + M_j^2} /Z$. These two are identical only if M_i or $M_j = 0$. The maximum discrepancy occurs where $M_i = M_j$ for which we obtain $\sigma = 2 C_2 M_i/Z$ vs. $\sqrt{2} C_2 M_i/Z$. Accordingly, use of the resultant moment can, for certain moment combinations, decrease the conservatism of the simplified analysis.

B₂-Indices

The B₂-indices are intended to represent an ultimate load as represented by the development of a plastic hinge through the body of the component. Neither theory nor test data exists for "limit" moments on branch connections in either heads or cylinders. Some theory and

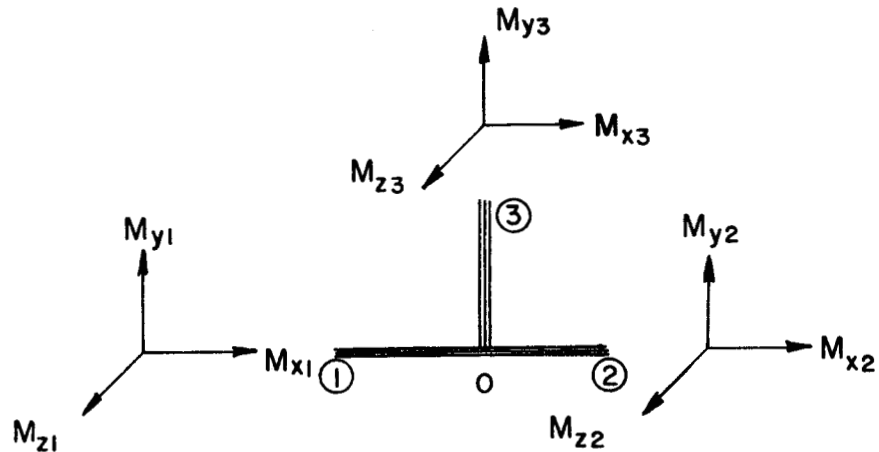
* Maximum here is with respect to location on the surface of the component, not maximum vs. minimum principal stress at a single point on the surface of the component.

test data^(18,19,20) indicate that the limit load on an elbow can be conservatively estimated by using 0.75 times the elastic stress index. That is, the elbow will collapse when the maximum elastic stress produced by the moment reaches 1.33 times the yield strength of the elbows material.

Because some analogy between elbows and full size tees was established by Markl⁽¹⁵⁾, and for lack of any better guidance, the proposed B_2 -indices for branch connections are also proposed to be 0.75 times the C_2 -indices for branch connections. A lower limit of $B_2 = 1.00$ is necessary to conform with the B_2 -indices for straight pipe. It is believed that these B_2 -indices are highly conservative but can be used in B31.7 because, at least so far, there have been no indications that Equation (9) of B31.7 presents a limitation to water-cooled reactor piping designs.

Summary and Example

The piping system flexibility analysis is assumed to give the sets of moments shown below:



$$M_b = \sqrt{M_{x3}^2 + M_{y3}^2 + M_{z3}^2}$$

$$\text{If } |M_{i3}| = |M_{i1}| + |M_{i2}|, \quad M_{ir} = 0$$

$$\text{If } M_{i3} < |M_{i1}| + |M_{i2}|, \quad M_{ir} = \text{smaller of } |M_{i1}| \text{ or } |M_{i2}|$$

where $i = x, y, \text{ or } z$

$$M_r = \sqrt{M_{xr}^2 + M_{yr}^2 + M_{zr}^2}$$

$$B_{2b} = 0.75 C_{2b} \text{ but not less than } 1.0$$

$$B_{2r} = 0.75 C_{2r} \text{ but not less than } 1.0$$

$$C_{2b} = 3 (R_m/T_r)^{2/3} (r'_m/R_m)^{1/2} (T'_b/T_r) (r'_m/r_p) \text{ but not less than } 1.5$$

$$K_{2b} = 1.0$$

$$C_{2r} = 0.8 (R_m/T_r)^{2/3} (r'_m/R_m)$$

$$K_{2r} = 2.0$$

The product of $C_{2r} K_{2r}$ shall be a minimum of 3.0

Moment loading terms of Equations (9), (10), (11), and (12)

of B31.7

$$\text{Eq. (9)} \quad S_{bM} = B_{2b} \frac{M_b}{Z_b} + B_{2r} \frac{M_r}{Z_r}$$

$$\text{Eq. (10) and (12)} \quad S_{nM} = C_{2b} \frac{M_b}{Z_b} + C_{2r} \frac{M_r}{Z_r}$$

$$\text{Eq. (11)} \quad S_{pM} = C_{2b} K_{2b} \frac{M_b}{Z_b} + C_{2r} K_{2r} \frac{M_r}{Z_r}$$

ExampleBranch Connection

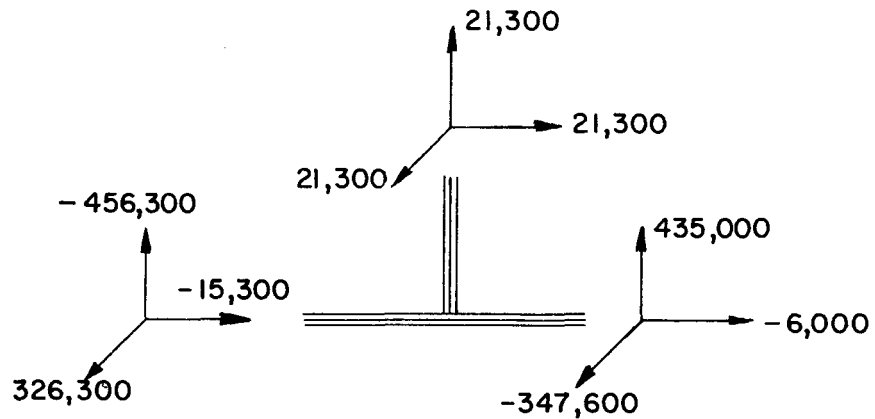
Run Pipe: 12.75" O.D. x 0.500" Wall; $R_m = 6.125"$, $T_r = 0.500"$

Branch Pipe: 4.50" O.D. x 0.237" Wall; $r'_m = 2.131"$, $T'_b = 0.237"$

Reinforcing: Weldolet as shown in Figure 3; $r_p = 2.90"$

Results from the Piping System Flexibility Analysis

For a loading condition applicable to Equation (10) and (11) of B31.7 the piping system is assumed* to give the moment ranges (in-lb) shown below

Stress Indices

$$B_{2b} = 0.75 \quad C_{2b} = 2.457$$

$$B_{2r} = 0.75 \quad C_{2r} = 1.110$$

} These are not used in this example.

$$C_{2b} = 3 \left(\frac{R_m}{T_r} \right)^{2/3} \left(\frac{r'_m}{R_m} \right)^{1/2} \left(\frac{T'_b}{T_r} \right) \left(\frac{r'_m}{r_p} \right) = 3.276$$

* These moments were chosen so that a 4" std. wt. long radius elbow in the branch pipe, subjected to M_{x3} , M_{y3} , M_{z3} , would have a stress of $2.8 S_m$ and a 12" X.S. long radius elbow in the run pipe, subjected to M_{x1} , M_{y1} , M_{z1} , would also have a stress of $2.8 S_m$, where $S_m = 17,300$ psi for A106 Gr B at 600 F.

$$K_{2b} = 1.0$$

$$C_{2r} = 0.8 (R_m/T_r)^{2/3} (r'_m/R_m) = 1.479$$

$$K_{2r} = 2.0$$

Calculation of M_b and M_r

$$M_b = \sqrt{21.3^2 + 21.3^2 + 21.3^2} \times 1000 = 36,893 \text{ in-lb}$$

$$|M_{x1}| + |M_{x2}| = |M_{x3}| \therefore M_{xr} = 0$$

$$|M_{y1}| + |M_{y2}| > M_{y3} \therefore M_{yr} = 435,000$$

$$|M_{z1}| + |M_{z2}| > M_{z3} \therefore M_{zr} = 326,300$$

$$M_r = \sqrt{0^2 + 435^2 + 326^2} \times 1000 = 543,780 \text{ in-lb}$$

Calculation of Secondary Stress for Moment Loading

$$S_{nM} = 3.276 \times \frac{36,893}{3.22} + 1.479 \times \frac{543,780}{56.7} = 51,719 \text{ psi}$$

(The value of S_{nM} is equal to $2.99 \times 17,300$ as compared to $2.8 \times 17,300$ for elbows under analogous moments. See footnote on preceding page.)

Calculation of Peak Stress for Moment Loading

$$S_{pm} = 3.276 \times 1.00 \times \frac{36,893}{3.22} + 3.0 \frac{543,780}{56.7} = 66,306 \text{ psi}$$

In the second term, $C_{2r}K_{2r} = 1.479 \times 2 = 2.958$ is less than 3.0, hence 3.0 is the required factor.

(Entering Fig. 1.705.3(a) of B31.7 with $S_{alt} = \frac{1}{2} S_{pM} = 33,150$
shows that the branch connection is suitable for up to 15,000
cycles of this particular loading.)

STRESSES BY B31.1.0 POWER PIPING CODE

Paragraph 119.6.4 from B31.1.0-1967 is reproduced herein as Figure 9. Paragraph (a) gives a set of rules which are directly applicable to elbows or curved pipe. Its use for straight tees requires some interpretation. Paragraph (b) gives equations for calculating S_b . Everything is defined adequately except Z which, in the preceding paragraph (a), is defined as "section modulus of pipe, in³". Presumably, as used in paragraph (b), Z is more specifically the section modulus of the run pipe. The author would interpret paragraph (b) as requiring the calculation of three values of S_b ; for run end 1, for run end 2, and for the branch. Now, presumably, one returns to paragraph (a), equation (8), to calculate S_E . The question arises as to what is S_t for M_t on the branch. Is it $M_{t3}/2Z$ or $M_{t3}/2Z_b$ or perhaps $M_t/2Z'_b$, where Z'_b is the actual section modulus of the branch pipe? These are minor points and could be cleared up with some editing. There are, however, some more basic questions concerning these code rules.

(1) Consider the moment M_{bt} acting alone on the branch. The bending

stress is either

$$(a) \quad S_b = \frac{i_{bt} M_{bt}}{\pi r_b^2 i_{bt} t_b} = \frac{M_{bt}}{Z_b} \quad \text{if } i_{bt} t_b < t_H$$

$$(b) \quad S_b = \frac{i_{bt} M_{bt}}{\pi r_b^2 t_H} = \frac{M_{bt}}{Z_b} i_{bt} \frac{t_b}{t_H} \quad \text{if } i_{bt} t_b > t_H$$

Case (a) gives a stress intensification factor of unity and forms a lower bound for case (b). One could accomplish the same thing by giving

119.6.4 Stresses.

(a) Calculations for the stresses shall be based on the least cross sectional area of the component, using nominal dimensions at the location of local strain. Calculations for the expansion stress, S_E , shall be based on the modulus of elasticity, E_C , at room temperature.

The expansion stresses shall be combined in accordance with Formula (8).

$$S_E = \sqrt{S_b^2 + 4S_t^2} \quad (8)$$

where

S_E = Computed expansion stress, psi

S_b = Resultant bending stress, psi =

$$\frac{\sqrt{(iM_{bp})^2 + (iM_{bt})^2}}{Z}$$

S_t = Torsional stress, psi = $\frac{M_t}{2Z}$

M_{bp} = Bending moment in plane of member, in. lb

M_{bt} = Bending moment transverse to plane of member, in. lb

M_t = Torsional moment, in. lb

Z = Sectional modulus of pipe, in.³

i = Stress intensification factor, Appendix D.

(b) Bending stresses for reduced outlet connections shall be calculated in accordance with the following equations, with moments as shown in Fig. 119.6.4(b).

S_b = Resultant bending stress, psi

$$= \frac{\sqrt{(i_{bp}M_{bp})^2 + (i_{bt}M_{bt})^2}}{Z} \quad \text{for Header (Legs 1 and 2)}$$

$$= \frac{\sqrt{(i_{bp}M_{bp})^2 + (i_{bt}M_{bt})^2}}{Z_b} \quad \text{for Branch (Leg 3)}$$

Z_b = Effective section modulus for branch of tee, in.³ = $\pi r_b^2 t_s$

r_b = Mean branch cross-sectional radius, in.

t_s = Effective branch wall thickness, in. = Lesser of T_H and $(i_{bt})(t_b)$

t_H = Thickness of pipe matching run of tee or header exclusive of reinforcing elements, in.

t_b = Thickness of pipe matching branch, in.

i_{bp} = Stress intensification factor for in plane bending moments = $0.75 i_{bt} + 0.25$

i_{bt} = Stress intensification factor for out of plane bending moments = i (Appendix D).

Allowable stress range, S_A , and permissible additive stresses shall be in accordance with those in Par. 102.3.2(c) and (d).

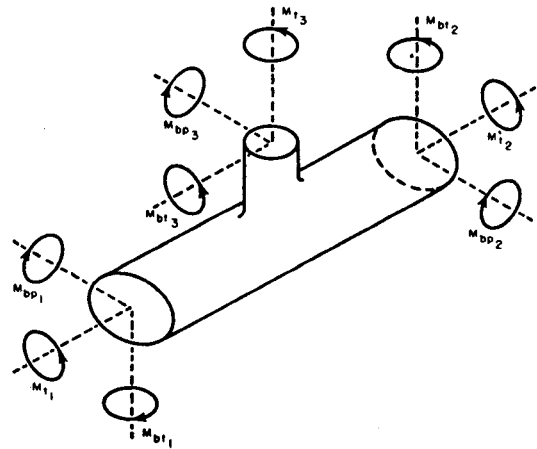


FIG. 119.6.4(b). REDUCING OUTLET CONNECTIONS.

only (b) with the restriction that $(i_{bt} t_b/T_H)$ shall not be taken as less than unity. One notes that for configurations where t_b/T_H is of the order of 1/3 or smaller, the stress intensification factor is likely to be unity. Comparisons of test data with the equation for case (b) indicate it may be unconservative⁽²¹⁾.

(2) The code rules assign a stress intensity factor of 1.00 for torsional moments but because the stress is considered as a shearing stress, this is equivalent to assigning a factor of 2.00 in relationship to stress intensity. Available test data raise some doubts as to whether this is conservative.

(3) If the code is properly interpreted as requiring an independent check of S_b for each of the three ends of the tee, using the set of moments at each of those ends, then any interaction between stresses from moments "through-the-branch" and moments "through-the-run" would be ignored. This would appear to be potentially unconservative for some configurations.

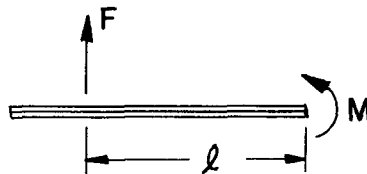
* * * * *

The above comments on B31.1.0 rules are not intended to be a serious criticism of those rules, since they are perhaps quite adequate for most piping systems, but rather to indicate why the author proposes a different set of rules for use in B31.7 for class 1 nuclear power piping.

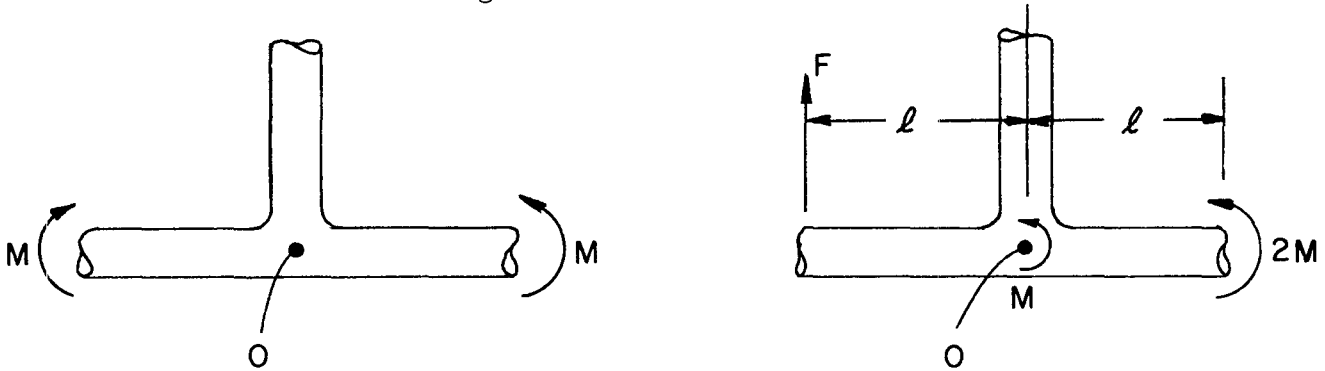
FORCE LOADINGS

At a branch intersection point, such as point "0" of Figure 2(a), the piping system analysis will give three orthogonal sets of forces in addition to the three sets of moments. The question arises as to what, if anything, should be done with these force loads. The piping system analysis assumes that these are forces at a point which, in terms of the actual shell configuration of branch connections, is not even a point on the physical structure. Accordingly, these forces have no direct physical significance. However, if we imagine these forces as existing in the pipe at some one or two pipe diameters from the run-branch axis intersection, some physical significance can be attached to the forces. Assuming these forces do exist some distance from the intersection point, it can be seen that only one pair of forces can exist without accompanying moments; that being $F_{x1} = -F_{x2}$; i.e., forces through the run pipe. For small d/D branch connections, the force F_{y3} reacted by F_{y1} and/or F_{y2} may exist without significant accompanying moments. The remaining forces will necessarily be accompanied by significant moments.

With respect to the moment-generating forces, it should be noted that the moment itself is included in the set of moments at point "0" of Figure 2(a). That is, an equilibrium requirement is $F\ell = M$.



The basic question is whether there are significant stresses in branch connections due to the shear force itself; e.g., would the stresses be different in the two loading conditions sketched below?



In ordinary beam theory (ignoring shear stresses), no difference in calculated stress would exist at point "O". Including shear stresses would give some difference; depending upon the ratio of depth to length of the beam. There is a little test data pertinent to the question. The test models of Table 1 were subjected to both force loads and moment loads. For these particular test models, no significant difference could be detected from the results. There are certain experimental difficulties associated with force-load tests. In order to detect the shear load effect it is desirable to introduce the shear force close to the branch connection. However, if we do so then the particular method of introducing the force will affect the stresses. For example, if we try to introduce the force uniformly around the pipe circumference through a ring, then that ring would stiffen the branch connection. A point load application might even more affect the measured stress. Accordingly, it is necessary to apply the force to the pipe some distance away from the branch; in this case the moment load is sufficiently large so that it effectively masks any stress due to shear

loading. A corrolary for actual piping systems is that unless there is an anchor close to a branch connection, the moment-generating forces will produce insignificant stresses as compared to the stresses produced by the moment. If an anchor is close to a branch connection, then the stresses (for both moment and force loads) will be dependent upon the geometry and closeness of that anchor; none of the data discussed herein would be applicable.

An axial force on the branch, F_{y3} , will produce a moment in the run pipe; its magnitude will depend upon how far out the reacting forces F_{y1} and F_{y2} are applied. There are some test data for F_{y3} loading listed opposite "L" of Table 3. The references do not indicate where or what kind of reactions were used. Presumably, the reactions were far enough from the branch connection so that they did not directly affect the stresses and close enough so that the moment in the run pipe was insignificant. One notes from Table 3 that the stress indices for axial force on the branch are larger than for any moment load. However, these are not indexed to the same nominal stress. To compare stresses* one may use the relation :

$$\frac{\sigma_f}{\sigma_m} = \frac{i_f F Z_b}{i_m M A_b} \approx \frac{i_f}{i_m} \frac{F}{M} \frac{r'_m}{2} \quad (13)$$

At most points in many typical piping systems, the moment M (in-lb) is 2 or more orders of magnitude greater than F (lbs), for which

* σ_f = stress due to force load

σ_m = stress due to moment load

points the value of σ_f would be negligible compared to σ_m . One can, of course, postulate a piping system with a branch connection at some point where the moments on the branch are of the same order, or even smaller than $F r'_m$; in which case a stress analysis considering only moments would be unconservative.

An axial load F_{x1} reacted by F_{x2} does not produce any moments and any stresses from this loading will not be reflected by a stress analysis considering moment loads only. There is a little test data of this type of loading from the models shown in Table 1. The stress indices for an axial force through the run were:

<u>Model</u>	<u>σ/S</u>	<u>\emptyset</u>	<u>Surface</u>	<u>Gage No.</u>
Steel, M'f'g A	1.89	0	I	18
Steel, M'f'g B	1.14	90°	I	56 & 58
Copper-Nickel, M'f'g A	1.12	-45°	I	106
Weldolet	2.96	90°	I	510

where

σ = maximum measured principal stress

$S = F/A$

F = axial force through the run

$A = \text{area of pipe} = 2\pi R_m T_r$

In summary of the discussion on force loadings.

(1) Forces F_{y1} , F_{z1} , F_{y2} , F_{z2} , F_{x3} , and F_{y3} , when applied two or more pipe diameters from the branch-run axis, generate significant moments; the stresses

due to the forces are probably small as compared to those due to the moment.

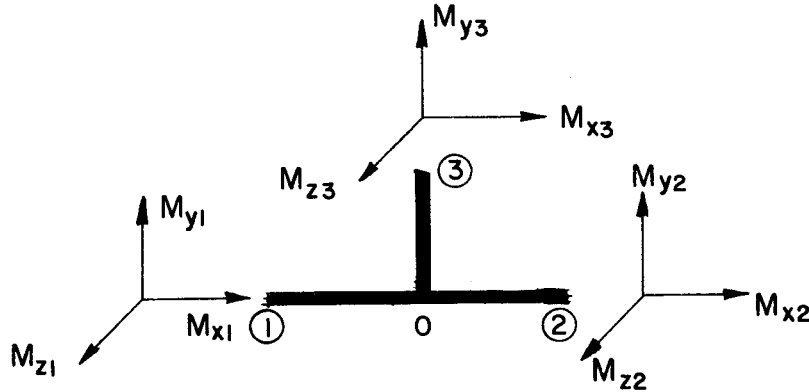
(2) Force F_{y3} , in small d/D branch connections, may produce a significant stress not included in stresses due to the accompanying moment through the run.

(3) Force F_{x1} , reacted by force F_{x2} , does not produce a moment. However, limited test data indicate these stresses will not be significant in most piping systems.

The author does not recommend inclusion of force loads in the B31.7 simplified analysis of stresses in branch connections. It is believed that the present factors and analysis are sufficiently conservative to compensate for possible stresses due to force loads. In this respect, the B31.7 analysis is equivalent to the B31.1.0 analysis, which also does not consider force loads in calculating stresses.

RECOMMENDED CHANGES IN B31.7Table D-201, Note (5), Branch Components

Replace present text and equations with the following.



Moments calculated for point at intersection of run and branch centerlines

$$M_b = \sqrt{M_{x3}^2 + M_{y3}^2 + M_{z3}^2}$$

$$\text{If: } |M_{i3}| = |M_{i1}| + |M_{i2}|, M_{ir} = 0$$

$$\text{If: } M_{i3} < |M_{i1}| + |M_{i2}|, M_{ir} = \text{smaller of } |M_{i1}| \text{ or } |M_{i2}|$$

where $i \equiv x, y, z$

$$M_r = \sqrt{M_{xr}^2 + M_{yr}^2 + M_{zr}^2}$$

For branch connections or tees, the M_i term or Equations (9), (10), (11), or (12) shall be calculated by the following pairs of terms.

$$\text{Equation (9)} \quad B_{2b} \frac{M_b}{Z_b} + B_{2r} \frac{M_r}{Z_r}$$

$$\text{Equations (10) \& (12)} \quad C_{2b} \frac{M_b}{Z_b} + C_{2r} \frac{M_r}{Z_r}$$

$$\text{Equation (11)} \quad C_{2b} K_{2b} \frac{M_b}{Z_b} + C_{2r} K_{2r} \frac{M_r}{Z_r}$$

where

$$Z_b = \pi (r'_m)^2 T'_b$$

$$Z_r = \pi R_m^2 T_r$$

For branch connections per subdiv. 1-704.3⁽³⁾:

r'_m , T'_b , R_m , and T_r are defined in Figure D-313

For butt-welding tees per USAS B16.9 or MSS SP 48:

r'_m = mean radius of designated branch pipe

T'_b = nominal wall thickness of designated branch pipe

R_m = mean radius of designated run pipe

T_r = nominal wall thickness of designated branch pipe

Table D-201, Note (7)

Replace with the following.

$$B_{2b} = 0.75 C_{2b} \text{ but not less than } 1.0$$

$$B_{2r} = 0.75 C_{2r} \text{ but not less than } 1.0$$

$$C_{2b} = 3(R_m/T_r)^{2/3} (r'_m/R_m)^{1/2} (T'_b/T_r)(r'_m/r_p), \text{ but not less than } 1.5.$$

R_m , T_r , r'_m , T'_b , and r_p are defined in Figure D-313.

$$K_{2b} = 1.0$$

$$C_{2r} = 0.8 (R_m/T_r)^{2/3} (r'_m/R_m), \text{ but not less than } 1.0$$

$$K_{2r} = 2.0$$

The product of $C_{2r} K_{2r}$ shall be a minimum of 3.0.

Table D-201, opposite "Branch connections per Subdiv. 1-704.3 and under column K_2

Replace "1.0" with "(7)".

Table D-201, Note (9)*

Replace with the following.

$$B_{2b} = B_{2r} = 0.75 C_{2b}$$

$$C_{2b} = C_{2r} = 0.67 (R_m/T_r)^{2/3}, \text{ but not less than 2.0.}$$

R_m = mean radius of designated run pipe

T_r = nominal wall thickness of designated run pipe

$$K_{2b} = K_{2r} = 1.0$$

Table D-201, Note (3)

Replace with the following.

The stress indices given are applicable only to branch connections in straight pipe with branch axes normal to the pipe surface and which meet the dimensional requirements and limitations of Par. D-313.1 and Figure D-313.

Figure D-313

Replace with Figure D-313 herein (page 60).

* This is a change in form, not in values; i.e., $1.8/(4.4)^{2/3} \approx 0.67$.

(This new figure is almost identical with Fig. 1-704.3.3.1. The differences are:

- (1) D-313 includes a definition of r_p
- (2) D-313 is applicable to both branches to pipe and branches in heads. The symbol, T_s , is used for either T_r (pipe) or T_h (head).
- (3) r_m and r_n are not shown because they are not involved in the stress indices.
- (4) d_o has been added to configuration (c). This is necessary for defining r_3 .

It should be noted that Par. D-313.1 gives limitations on corner and transition radii which are not included in 1.704.3.)*

Par. D 313.1 (e)

Change r_m to r'_m .

Par. D 313.1 (g)

Change last part from "... larger of $t/2$ or T_s^2 " to larger of $T_b/2$, $(T_b + y)/2$ [for Fig. D-313 (c)] or $T_s/2$.

Par. D-313.2

Change r_m to r'_m

Change t_b to T'_b

Add "y" to the list of symbols which "are defined in Figure D-313".

* This parenthetical note is not to be included in B31.7.

REFERENCES

- (1) USAS B31.7, Nuclear Power Piping, February 1968, Issued for Trial Use and Comment, Published by the American Society of Mechanical Engineers, 345 E. 47th St., New York, New York 10017.
- (2) Fung, F. K. and Lind, N. C., "Experimental Stress Analysis of a 45-degree Lateral Branch Pipe Connection Subjected to External Loadings", University of Waterloo, Waterloo, Ontario, Canada, September 1968.
- (3) Schoessow, G. J. and Kooistra, L. F., "Stresses in a Cylindrical Shell Due to Nozzle or Pipe Connection", ASME Journal of Applied Mechanics, June, 1945.
- (4) Jackson, et. al., "Stresses in Unreinforced Branch Connections", Battelle Memorial Institute Report to the American Gas Association, September 30, 1953.
- (5) Mehringer, F. J., and Cooper, W. E., "Experimental Determinations of Stresses in the Vicinity of Pipe Appendages to a Cylindrical Shell", S.E.S.A. Proceedings, XIV, (2), 1957.
- (6) Lane, P.H.R. and Rose, R. T., "Design of Welding Pipe Fittings", British Welding Research Association, Abington Hall, Abington, Cambridge, November, 1959.
- (7) Cranch, E. T., "An Experimental Investigation of Stresses in the Neighborhood of Attachments to a Cylindrical Shell", Welding Research Council Bulletin No. 60, May, 1960.
- (8) Hardenbergh, Zamrik and Edmondson, "Experimental Investigation of Stresses in Nozzles in Cylindrical Pressure Vessels", Welding Research Council Bulletin No. 89 (July, 1963).
- (9) Riley, W. F., "Experimental Determination of Stress Distributions in Thin-Walled Cylindrical and Spherical Pressure Vessels with Circular Nozzles", Welding Research Council Bulletin No. 108 (Sept., 1965).
- (10) McClure, G. M., Sweeney, J. A., and Gross, H. J., "Investigation of Stresses in Pipeline Branch Connections", Battelle Memorial Institute Report to the American Gas Association, March 30, 1956.
- (11) Rodabaugh, E. C., "Cyclic Bending Tests of a Half-Scale Model of an 8" x 24" Saddle Reinforced Branch Connection", Tube Turns (Div. of Chemetron) Report No. 8.011, Louisville, Ky., 1953.
- (12) Mills, E. J., Atterbury, T. J., and McClure, G. M., "Study of Effects of Cyclic Bending Loads on Performance of Branch Connections", Battelle Memorial Institute Report to the American Gas Association, Columbus, Ohio, May, 1962.

- (13) Pickett, A. G., et. al., "Low Cycle Fatigue Testing of One-Half Scale Model Pressure Vessels", Progress Reports No. 9 through 12, July, 1964 through January 1965. Southwest Research Institute, San Antonio, Texas (Contract No. AT(11-1)-1228, U.S. Atomic Energy Commission)
- (14) Rodabaugh, E. C., et. al., "Evaluation of Experimental and Theoretical Data on Radial Nozzles in Pressure Vessels", TID-24342.
- (15) Markl, A.R.C., "Fatigue Tests of Piping Components", Trans. ASME, Vol. 74, pp. 287-303 (1952).
- (16) Wichman, K. R., Hopper, A. G., and Mershon, J. L., "Local Stresses in Spherical and Cylindrical Shells Due to External Loadings", Welding Research Council Bulletin No. 107, August 1965.
- (17) Bijlaard, P. P., "Stresses from Local Loadings in Cylindrical Pressure Vessels", Trans. ASME (August 1955).
- Bijlaard, P. P., "Stresses from Radial Loads and External Moments in Cylindrical Pressure Vessels", Welding Research Supplement(Dec., 1955).
- Bijlaard, P. P., "Additional Data on Stresses in Cylindrical Shells Under Local Loading", Welding Research Council Bulletin No. 50 (May, 1959).
- (18) Marcal, P. V., "Elastic-Plastic Behavior of Pipe Bends with In-Plane Bending", J. of Strain Analysis, Vol. 2, No. 1, pp. 84-90 (1967).
- (19) Gross, N., "Experiments on Short Radius Pipe Bends", Proc. Instn. Mech. Engrs., Vol. 1B, p. 465 (1952-1953).
- (20) Gross, N. and Ford, H., "The Flexibility of Short-Radius Pipe Bends", Proc. Instn. Mech. Engrs., Vol. 1B, p. 480 (1952-1953).
- (21) Rodabaugh, E. C., "Flexibility and Stress Intensification Factors of Piping Components with Moment Loading", Battelle report to the American Gas Association, Oct. 21, 1966.

INTERNAL DISTRIBUTION

- | | | | |
|--------|-------------------|--------|-------------------------------|
| 1. | S. E. Beall | 28. | R. E. MacPherson |
| 2. | H. W. Behrman | 29. | H. C. McCurdy |
| 3. | M. Bender | 30. | J. G. Merkle |
| 4. | J. P. Blakely | 31. | A. J. Miller |
| 5. | S. E. Bolt | 32. | E. C. Miller |
| 6. | R. H. Bryan | 33-37. | S. E. Moore |
| 7. | J. W. Bryson | 38. | Paul Nelson |
| 8. | J. R. Buchanan | 39. | A. M. Perry |
| 9. | J. P. Callahan | 40. | C. E. Pugh |
| 10. | D. W. Cardwell | 41. | M. W. Rosenthal |
| 11. | J. M. Corum | 42. | A. W. Savolainen |
| 12. | W. B. Cottrell | 43. | M. J. Skinner |
| 13. | F. L. Culler | 44. | J. E. Smith |
| 14. | W. G. Dodge | 45. | I. Spiewak |
| 15. | M. H. Fontana | 46. | D. A. Sundberg |
| 16. | A. P. Fraas | 47. | D. B. Trauger |
| 17. | W. R. Gall | 48. | R. S. Valachovic |
| 18. | D. L. Gray | 49. | A. M. Weinberg |
| 19-20. | B. L. Greenstreet | 50. | G. D. Whitman |
| 21. | R. C. Gwaltney | 51. | F. J. Witt |
| 22. | W. O. Harms | 52. | G. T. Yahr |
| 23. | P. N. Haubenreich | 53-54. | Central Research Library |
| 24. | P. R. Kasten | 55-56. | Document Reference Section |
| 25. | K. C. Liu | 57-66. | Laboratory Records Department |
| 26. | M. I. Lundin | 67. | Laboratory Records (RC) |
| 27. | R. N. Lyon | | |

EXTERNAL DISTRIBUTION

68. R. W. Aderholdt, Auburn University, Auburn, Alabama
69. D. E. Allwein, Naval Ship Research and Development Center, Annapolis, Maryland
70. L. E. Alsager, USAEC, Washington, D.C.
71. R. L. Anderson, Pennsylvania Power and Light Co., Allentown, Penna.
72. W. F. Anderson, Liquid Metal Engineering Center, Canoga Park, Calif.
73. N. Balai, Argonne National Laboratory, Argonne, Illinois
74. R. E. Ball, Byron Jackson Pump, Inc., Los Angeles, Calif.
75. R. E. Benson, Tube Turns Corp., Louisville, Kentucky
76. D. J. Bergman, 683 Locust Road, Winnetka, Illinois
77. Irwin Berman, Foster Wheeler Corp., Livingston, New Jersey
78. Norman Blair, Ralph M. Parsons Co., Los Angeles, Calif.
79. F. J. Bogden, Westinghouse Electric Corp., Cheswick, Penna.
80. M. Booth, DRDT, USAEC, Washington, D.C.

81. E. B. Branch, Sargent and Lundy, Chicago, Illinois
82. H. F. Brannon, Yankee Atomic Electric Co., Boston, Massachusetts
83. M. N. Bressler, Taylor Forge, Inc., Wilmington, Delaware
84. W. E. Bristow, Monsanto Co., St. Louis, Missouri
85. G. O. Bright, Idaho Nuclear Corp., Idaho Falls, Idaho
86. R. Broadhead, Westinghouse Electric Corp., Pittsburgh, Penna.
87. J. E. Brock, U.S. Naval Postgraduate School, Monterey, Calif.
88. D. R. Campbell, Liquid Metal Engineering Center, Canoga Park, Calif.
89. L. H. Carr, Route 1, Box 170, San Luis Obispo, California
90. J. A. Casner, Youngstown Sheet and Tube Co., Youngstown, Ohio
91. J. R. Chamberlain, Borg-Warner Corp., York, Penna.
92. C. H. Chen, Auburn University, Auburn, Alabama
93. D. C. Church, General Dynamics Corp., Groton, Connecticut
94. J. R. Clapp, Burns and Roe, Inc., Hempstead, New York
95. R. L. Cloud, Teledyne Materials Research Co., Waltham, Massachusetts
96. R. W. Clough, University of California, Berkeley, Calif.
97. W. S. Clouser, Los Alamos Scientific Laboratory, Los Alamos, N.M.
98. R. H. Clute, Interprovincial Pipe Line Co., Edmonton, Alberta, Canada
99. John Conway, U.S. Navy Department, Bureau of Ships Code 609.3C, Washington, D.C.
100. W. E. Cooper, Teledyne Materials Research Co., Waltham, Massachusetts
101. L. M. Corcoran, MPR Associates, Inc., Washington, D.C.
102. J. E. Corr, General Electric Co., San Jose, California
103. H. T. Corten, University of Illinois, Urbana, Illinois
104. A. W. Crittenden, Niagara Mohawk Power Corp., Buffalo, New York
105. A. J. del Buono, Taylor Forge and Pipe Works, Chicago, Illinois
106. R. W. Dickinson, Liquid Metal Engineering Center, Canoga Park, Calif.
107. R. J. Dohrmann, Babcock and Wilcox Research Center, Alliance, Ohio
108. H. W. Dolfi, Combustion Engineering, Inc., Chattanooga, Tenn.
109. W. L. Dornaus, Bechtel Corp., San Francisco, Calif.
110. F. W. Dunham, David Taylor Model Basin, Code 703.1, Washington, D.C.
111. A. J. Edmondson, University of Tennessee, Knoxville
112. G. R. Edwards, Pittsburgh Des Moines Steel Co., Pittsburgh, Penna.
113. R. W. Elkins, Byron Jackson Pump, Inc., Los Angeles, Calif.
114. F. E. Ellyin, University of Sherbrooke, Sherbrooke, Canada
115. E. P. Esztergar, 6046 Bellevue Avenue, La Jolla, Calif.
116. J. R. Farr, Babcock and Wilcox Co., Barberton, Ohio
117. J. H. Faupel, E. I. du Pont de Nemours and Co., Wilmington, Delaware
118. D. M. Fischer, Amoco Chemicals Corp., Chicago, Illinois
119. J. D. Fishburn, Combustion Engineering, Inc., Windsor, Connecticut
120. R. H. Gallagher, Cornell University, Ithaca, New York
121. J. W. Gascoyne, C. F. Braun and Co., Alhambra, Calif.
122. H. H. George, Tube Turns, Inc., Louisville, Kentucky
123. J. C. Gerdeen, Michigan Technological University, Houghton, Michigan
124. E. F. Gerwin, M. W. Kellogg Co., Williamsport, Penna.
125. J. D. Gilman, General Electric Co., San Jose, Calif.
126. A. B. Glickstein, General Dynamics Corp., Groton, Connecticut
127. C. T. Grace, University of New Mexico, Albuquerque, N.M.
128. G. R. Graves, C. F. Braun and Co., Covina, California
129. R. C. Green, Southwest Fabricating and Welding Co., Houston, Texas
130. D. K. Greenwald, Ladish Co., Cudahy, Wisconsin
131. Bill Griffith, Bechtel Corp., San Francisco, Calif.

132. J. H. Griffin, Los Alamos Scientific Laboratory, Los Alamos, N.M.
133. S. C. Grigory, Southwest Research Institute, San Antonio, Texas
134. John Grund, Portland General Electric Co., Portland, Oregon
135. O. Hagen, Westinghouse Electric Corp., Cheswick, Penna.
136. E. E. Hamer, Argonne National Laboratory, Argonne, Illinois
137. E. E. Hay, Imperial Chemical Industries, Manchester 9, England
138. K. Hayashi, Esso Research and Engineering Co., Florham Park, N.J.
139. J. K. Hayes, Combustion Engineering, Inc., Chattanooga, Tenn.
140. D. B. Heilig, Bechtel Corp., San Francisco, Calif.
141. T. K. Hellen, Berkeley Nuclear Laboratories, Berkeley, England
142. R. W. Holland, University of Tennessee, Knoxville, Tenn.
143. R. J. Hollmeier, Pioneer Service and Engineering Co., Chicago, Ill.
144. A. B. Holt, USAEC, Washington, D.C.
145. F. I. Horan, NASA Langley Field, Hampton, Virginia
146. J. P. Houstrup, Combustion Engineering, Inc., Chattanooga, Tenn.
147. L. L. Hsu, General Electric Corp., San Jose, Calif.
148. K. A. Huber, Byron Jackson Pump, Inc., Los Angeles, Calif.
149. L. E. Hulbert, Battelle Memorial Institute, Columbus, Ohio
150. H. Huner, Auburn University, Auburn, Alabama
151. J. R. Hunter, RDT, USAEC, Washington, D.C.
152. R. W. Jackson, National Valve and Manufacturing Co., Pittsburgh, Pa.
153. M. T. Jakub, Battelle-Northwest Laboratory, Richland, Washington
154. R. I. Jetter, Atomics International, Canoga Park, Calif.
155. R. L. Johnson, Westinghouse Electric Corp., Pittsburgh, Penna.
156. A. W. Jones, Rolls Royce and Associates, Ltd., Derby, England
157. Ralph Jones, USAEC, Washington, D.C.
158. S. M. Jorgensen, Foster Wheeler Corp., Livingston, New Jersey
159. L. M. Kaldor, U. S. Navy, Annapolis, Maryland
160. R. J. Kiessel, U. S. Coast Guard, 1300 E Street, Washington, D.C.
161. E. E. Kintner, RDT, USAEC, Washington, D.C.
162. W. G. Knecht, Darling Valve and Mfg. Co., Williamsport, Penna.
163. Robert Koester, The Wm. Powell Co., Cincinnati, Ohio
164. Z. A. Kravets, Consolidated Edison Co. of New York, New York, N.Y.
165. N. Krishnamurthy, Auburn University, Auburn, Alabama
166. D. F. Landers, Teledyne Materials Research Co., Waltham, Massachusetts
167. G. Landler, Atomics International, Canoga Park, Calif.
168. E. P. Lang, Lunkenheimer Co., Cincinnati, Ohio
169. D. F. Lange, USAEC, Washington, D.C.
170. B. F. Langer, Westinghouse Electric Corp., Pittsburgh, Penna.
171. C. F. Larson, Welding Research Council, 345 E. 47th St., New York, N.Y.
172. R. E. Lawther, Westinghouse Electric Corp., Pittsburgh, Penna.
173. M. M. Lemcoe, Liquid Metal Engineering Center, Canoga Park, Calif.
174. M. R. Lesh, Esso Research and Engineering Co., Florham Park, N.J.
175. M. M. Leven, Westinghouse Electric Corp., Pittsburgh, Penna.
176. M. J. Letich, American Bureau of Shipping, New York, N.Y.
177. G. E. Lien, American Electric Power Service Corp., New York, N.Y.
178. N. C. Lind, University of Waterloo, Waterloo, Ontario, Canada
179. R. G. Lloyd, Babcock and Wilcox Co., Barberton, Ohio
180. A. Lohmeier, Westinghouse Electric Corp., Tampa, Florida
181. R. H. Luhta, Darling Valve and Manufacturing Co., Williamsport, Penna.
182. George McClure, Battelle Memorial Institute, Columbus, Ohio

183. C. M. McCullar, Bechtel Corp., San Francisco, Calif.
184. J. T. McKeon, M. W. Kellogg Co., Piscataway, New Jersey
185. N. R. McKinney, Southern Services, Inc., Birmingham, Alabama
186. W. N. McLean, Crane Co., Chicago, Illinois
187. G. R. McNutt, Tennessee Valley Authority, Knoxville, Tenn.
188. E. A. McPhillamy, Sandusky Foundry and Machine Co., Sandusky, Ohio
189. J. B. Mahoney, Applied Technology Associates, L.I., New York, N.Y.
190. L. J. Malandra, Westinghouse Electric Corp., Pittsburgh, Penna.
191. M. V. Malkmus, Tube Turns, Louisville, Kentucky
192. J. R. Maloney, Westinghouse Electric Corp., Cheswick, Penna.
193. M. J. Manjoine, Westinghouse Electric Corp., Pittsburgh, Penna.
194. W. D. Manly, Union Carbide Corporation, Kokomo, Indiana
195. Pedro Marcal, Brown University, Providence, Rhode Island
196. L. P. Marchesani, Sun Oil Co., Philadelphia, Penna.
197. A. Mathews, University of Tennessee, Knoxville, Tenn.
198. J. D. Mattimore, 3130 Meadowlark Road, Louisville, Kentucky
199. J. M. Matusz, Rockwell Manufacturing Co., Pittsburgh, Penna.
200. R. L. Maxwell, University of Tennessee, Knoxville, Tenn.
201. J. L. Mershon, RDT, USAEC, Washington, D.C.
202. W. R. Mikesell, Chicago Bridge and Iron Co., Oak Brook, Illinois
203. C. E. Miller, Jr., Argonne National Laboratory, Argonne, Illinois
204. B. J. Milleville, Rockwell Manufacturing Co., Pittsburgh, Penna.
205. A. T. Molin, United Engineers and Constructors, Philadelphia, Penna.
206. C. L. Moon, Atomic Energy of Canada, Ltd., Ontario, Canada
207. C. A. Moore, Idaho Nuclear Corp., Idaho Falls, Idaho
208. J. K. Morse, Combustion Engineering, Inc., Chattanooga, Tenn.
209. I. Mortman, General Electric Co., KAPL, Schenectady, N. Y.
210. E. D. Mysinger, Tennessee Valley Authority, Knoxville, Tenn.
211. A. D. Nalbandian, Grinnell Corp., Providence, Rhode Island
212. R. M. Nelson, Bingham-Willamette Co., Portland, Oregon
213. D. J. Nolan, United Nuclear Corp., Elmsford, New York
214. W. J. O'Donnell, O'Donnell and Associates, 3611 Maplevue Drive, Bethel Park, Penna.
215. E. T. Onat, Yale University, New Haven, Conn.
216. J. A. Paget, Gulf General Atomic, Inc., San Diego, Calif.
217. D. H. Pai, Foster Wheeler Corp., Livingston, New Jersey
218. M. Pakstys, General Dynamics, Groton, Connecticut
219. W. B. Palijenko, Ontario Hydro, Toronto 2, Ontario, Canada
220. A. J. Palmer, Esso Research and Engineering Co., Florham Park, N.J.
221. G. W. Pangborn, Combustion Engineering, Inc., Windsor, Conn.
222. C. T. Parker, General Electric Co., San Jose, Calif.
223. G. L. Parkinson, Bechtel Corp., San Francisco, Calif.
224. N. T. Peters, Giffels and Rosetti, Inc., Detroit, Michigan
225. D. B. Peterson, KPA Computer Techniques, Inc., Large, Penna.
226. A. G. Pickett, Southwest Research Institute, San Antonio, Texas
227. D. L. Platus, Mechanics Research, Inc., El Segundo, Calif.
228. R. W. Pochmann, U. S. Industries, Inc., Houston, Texas
229. J. J. Poer, Commonwealth Edison Co., Chicago, Illinois
230. C. H. Powell, University of California, Berkeley, Calif.
231. A. J. Pressesky, USAEC, Washington, D.C.

232. J. C. Quinn, Lunkenheimer Co., Cincinnati, Ohio
233. F. C. Rally, General Electric Co., Sunnyvale, Calif.
234. Y. R. Rashid, General Electric Co., San Jose, Calif.
235. G. S. Rasmussen, G. S. Rasmussen and Associates, Glendale, Calif.
236. R. T. Reid, Aerojet Nuclear Systems Co., Sacramento, Calif.
237. B. Roberts, Combustion Engineering, Inc., Chattanooga, Tenn.
238. E. C. Rodabaugh, Battelle Memorial Institute, Columbus, Ohio
239. O. A. Rogers, Y-12 Plant, Oak Ridge, Tenn.
240. M. A. Rosen, DRDT, USAEC, Washington, D.C.
241. G. S. Rosenberg, Argonne National Laboratory, Argonne, Illinois
242. H. D. Ross, Babcock and Wilcox Co., Lynchburg, Virginia
243. B. J. Round, Combustion Engineering, Inc., Windsor, Connecticut
244. E. J. Rozic, Babcock and Wilcox Co., Beaver Fall, Penna.
245. V. L. Salerno, 2430 Laconia Avenue, Bronx, New York
246. R. F. Sammataro, General Dynamics Corp., Groton, Connecticut
247. Robert Schmidt, Ladish Co., Cudahy, Wisconsin
248. W. R. Schmidt, MPR Associates, Inc., Washington, D.C.
249. R. W. Schneider, Bonney Forge and Foundry, Inc., Allentown, Penna.
250. J. J. Schreiber, USAEC, Washington, D.C.
251. J. Schroeder, University of Waterloo, Waterloo, Ontario, Canada
252. J. G. Schumacher, Aerojet-General Corp., Sacramento, Calif.
253. H. R. Selby, Bechtel Corp., Gaithersburg, Maryland
254. Jagmohan Seoni, Bechtel Corp., Gaithersburg, Maryland
255. W. A. Shaw, Auburn University, Auburn, Alabama
256. R. L. Shively, General Electric Co., San Jose, California
257. V. Skoglund, University of New Mexico, Albuquerque, N.M.
258. R. J. Slember, United Nuclear Corp., Elmsford, N.Y.
259. H. B. Smith, Combustion Engineering, Inc., Windsor, Connecticut
260. W. R. Smith, Sr., Bechtel Corp., San Francisco, Calif.
261. A. L. Snow, Westinghouse Electric Corp., Madison, Pennsylvania
262. R. E. Soderberg, Walworth Co., Greenburg, Penna.
263. J. E. Soehrens, C. F. Braun and Co., Alhambra, Calif.
264. J. L. V. Sperry, Detroit Edison Co., Detroit, Michigan
265. E. D. Ssinegurski, Combustion Engineering, Inc., Windsor, Connecticut
266. R. E. Stanbridge, Liquid Metal Engineering Center, Canoga Park, Calif.
267. E. H. Steigerwald, Bechtel Corp., Gaithersburg, Maryland
268. K. O. Stein, Babcock and Wilcox Co., Alliance, Ohio
269. R. G. Sturm, Teledyne-Brown Engineering, Huntsville, Alabama
270. W. H. Sutherland, Battelle-Northwest Laboratory, Richland, Wash.
271. E. O. Swain, General Electric Co., San Jose, Calif.
272. W. F. Swinson, Auburn University, Auburn, Alabama
273. S. W. Tagart, General Electric Co., San Jose, Calif.
274. R. E. Taylor, Reinhold Publishing Co., Chicago, Illinois
275. B. E. Tenzer, Ebasco Services, Inc., New York, N.Y.
276. R. E. Tschirch, Hartwell Company, Inc., East Providence, Rhode Island
277. W. H. Tuppeny, Combustion Engineering, Inc., Windsor, Connecticut
278. A. B. van Weelderren, Westinghouse Electric Corp., Tampa, Florida
279. F. E. Vinson, Bechtel Corp., San Francisco, Calif.
280. E. O. Waters, 28F Heritage Village, Southbury, Connecticut
281. R. F. Webster, U. S. Steel Corp., Pittsburgh, Penna.

282. B. Wei, RDT, USAEC, Washington, D.C.
283. K. R. Wichman, Navy Department, Washington, D.C.
284. F. S. G. Williams, 5555 N. Sheridan Road, Chicago, Illinois
285. L. E. Wright, C. F. Braun and Co., Alhambra, Calif.
286. W. B. Wright, Westinghouse Electric Corp., Pittsburgh, Penna.
287. J. N. Wu, Babcock and Wilcox Co., Alliance, Ohio
288. G. Y. Young, Niagara Mohawk Power Corp., Buffalo, N.Y.
289. J. C. M. Yu, Auburn University, Auburn, Alabama
290. Lin Yung-Lo, Bliss R and D Co., Swarthmore, Penna.
291. S. Y. Zamrik, Pennsylvania State Univ., University Park, Penna.
292. Zenons Zudans, Franklin Institute Research Labs, Philadelphia, Pa.
293. M. P. Zyne, Southern Services, Birmingham, Alabama
294. Librarian, Bechtel Corp., Gaithersburg, Maryland
295. NRTS Technical Library, P. O. Box 1845, Idaho Falls, Idaho
296. Librarian, Westinghouse Electric Corp., Pittsburgh, Penna.
- 297-311. Division of Technical Information Extension (DTIE)
312. Laboratory and University Division, ORO